Determination of Maximum Safe Depth of Unsupported Excavation Pit and Minimum Safe Horizontal Distance from Adjacent Foundations

MS GEOTECHNICAL ENGINEERING THESIS

DISSERTATION

By

Muhammad Hamza Khalid

Reg No: 00000319747

Supervisor

Dr. Badee Alshameri

NUST Institute of Civil Engineering

School of Civil and Environmental Engineering

National University of Sciences and Technology, Islamabad, Pakistan

2022

This is to certify that thesis titled

Determination of Maximum Safe Depth of Unsupported Excavation Pit and Minimum Safe Horizontal Distance from Adjacent Foundations

Submitted by

MUHAMMAD HAMZA KHALID

Fall 2019 MS-Geotechnical Engineering

00000319747

has been accepted towards the partial fulfilment of the

requirements for the award of degree

of

Master of Science in Geotechnical Engineering

_____

Dr. Badee Alshameri (Supervisor)

HoD Geotechnical Engineering

NUST Institute of Civil Engineering (NICE)

School of Civil and Environmental Engineering (SCEE)

National University of Sciences and Technology (NUST), Islamabad, Pakistan

Thesis Acceptance Certificate

It is certified that final copy of MS thesis written by **Mr. Muhammad Hamza Khalid**, Registration No. **00000319747**, of MS Geotechnical Engineering 2019 Batch (NICE), has been vetted by undersigned, found completed in all respects as per NUST Statutes/Regulations, is free of plagiarism, errors, and mistakes and is accepted as partial fulfillment for award of **MS degree in Geotechnical Engineering**.

Signature_____

Supervisor: Dr. Badee Alshameri

Head of Department

Date: _____

Signature_____

Dean: Dr. Syed Muhammad Jamil

Date: _____

Dedication

This research is dedicated to my parents Dr. Muhammad Yousaf Khalid and Dr. Gul Nasreen who have loved and nourished me unconditionally; my siblings Junaid and Noor who are my best friends; my mentor Dr. Badee Alshameri who encouraged me to push my limits and strengthened my belief that darkness doesn't last forever and Dr. S.M. Jamil; to whom I look up to.

Acknowledgements

My colleagues and class fellows have been a source of constant encouragement. I would acknowledge members of Survey Lab (NICE) who made my academic tenure comfortable. Lt. Col. Nasrul Haq who pushed me to gain new insight, trained and polished me. I am in gratitude of Mr. Mehmood who helped in data collection and convinced local people to co-operate for the study.

Abstract

Unsupported excavations are very common in Pakistan for foundation construction. Design aids or statutory laws to ensure safe excavation practices do not exist. Unsupported excavations pose settlement, distortion, and pit face failure threats to adjacent buildings. The study intends to find the range of influence zone of unsupported excavations. Data was collected from 44 sites in Mirpur Azad Kashmir, Pakistan. The parameters collected included excavation depth, distance of structures from excavation; foundation width and load of the adjacent building; unit weight, cohesion, and elastic modulus of the soil. Three Machine Learning (ML) models i.e., Multi-layer Perceptron (MLP), Gene Expression Programming (GEP) and Decision Tree (DT) were trained to predict if a combination of the seven parameters was safe against stability damage. MLP model showed maximum accuracy of 89%. The average of the influence ranks from Garson 1991 method and local sensitivity analysis deemed unit weight and elastic modulus as the least influential parameters. The remaining 5 parameters were taken as variables to be modelled in PLAXIS to produce design charts. The most recurrent values from the dataset were taken as inputs. 15 design charts were made incorporating cohesion values 5, 10 and 15 kPa; foundation widths of 7.5, 10, 13.5,16 and 20 meters and loads of 10, 20 and 30 kPa. To get comparable design charts, MLP model was provided with the same inputs as well. Design charts from both approaches were validated against 14 case studies. The accuracy of PLAXIS and MLP design charts proved to be 78.6% and 85.7% respectively. The MLP model and design charts are recommended for safe practice of unsupported excavation for residential units in soft homogenous soils.

Table of Contents

List of Figures

List of Tables

CHAPTER 1

INTRODUCTION

1.1   Background

The rapid urbanization of present age has induced the need of efficient use of space for buildings and infrastructures, this in turn has led to vertical sprawl in buildings. The exponential increase in population, inclination towards urban agglomeration for fostering urban synergy among diverse activities and specialized services, expensive land prices and need for less travelling are few among the reasons for the shift towards multistorey buildings in urban centers (Al-Kodmany, 2012). Much emphasis has been laid for achieving sustainability objectives by increasing number of dwelling units per acre (Toderian, 2011). The confined spaces in urban centers have compelled planners to construct buildings adjacent to each other. During excavations, the stability and ground movements are the major concerns as these are inter-related. It means that factors affecting the performance of excavations will also affect ground stability and the structures on it. Therefore, it is important to know what these factors are and how they affect the performance. The excavations for foundations with unsupported vertical cuts are common in Pakistan. These pose threats to stability of existing adjacent buildings (Zhang et al., 2018). The instability of existing buildings due to adjacent excavation can arise due to three reasons.

1) Differential settlement of foundation due to pit excavations (Zhang, 2020),

2) Distortion of foundation (Burland & Wroth, 1974) and

3) Failure of excavation pit face similar to slope stability failures (Wang et al., 2020)(Hu & Ma, 2018).

Critical unsupported excavation depths have been provided by various researchers and construction guidelines are being practiced throughout the world (Karl, 1866; Fellenius, 1927; Irfan et al., 2013; Aljorany & Al-qaisee, 2018; Antinoro et al., 2017; Bakr, 2019; Richard et al., 2019). However not all failure criteria have been considered. Moreover, surcharge from adjacent buildings, distance to adjacent buildings, foundation size and major strength properties of soils have also not been considered.

1.2 Problem Statement

Critical unsupported excavation depth in clays have been proposed (Karl, 1866,Fellenius, 1927,Terzaghi, 1943), however the surcharge form adjacent buildings, foundation size, distance from the excavation and major soil parameters have not been considered. Studies have been performed by researchers solely to determine the safe excavation depths in clays and sands (Irfan et al., 2013,Aljorany & Al-qaisee, 2018,Richard et al., 2019, Bakr, 2019, Brennan et al., 2020) by incorporating soil properties and load however not all damage evaluation criteria have been considered to provide horizontal range of influence of unsupported excavations. In open cut excavations, there is no support provided to the walls of the pit. The movement of soil mass causes settlement cracks in the existing structure and can cause lateral soil flow. In developing nations like Pakistan, unsupported excavations are very common in the construction of residential units. The structural, aesthetical and serviceability damages require costly repairs and expensive preventive measures to stop further damage. Therefore, a guide to determine the safe depth of unsupported excavation and lateral distance from the existing structures is crucial. The problem is illustrated in figure 1.1.
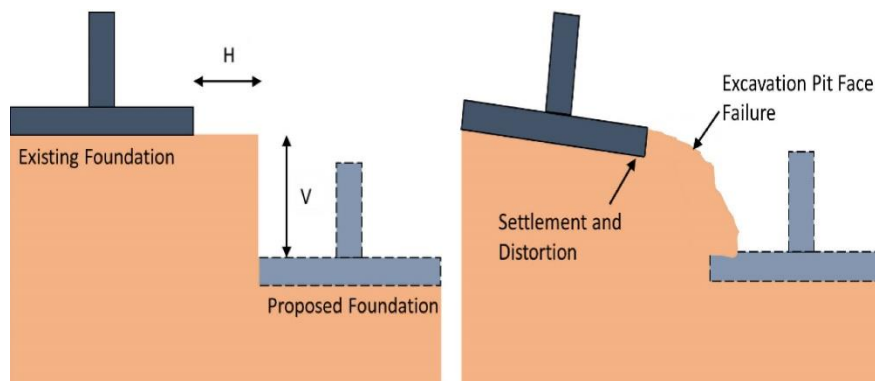
Figure 1.1 Illustration of Problem Statement

1.3 Aims and Objectives

The aim of this research is to develop design charts and aids for safe unsupported excavation practices adjacent to residential buildings. The aim can be achieved by the following objectives:

- Development of a database from precedents for foundation pit depth for new structures, horizontal distance from an existing building, existing building load and foundation dimensions, soil properties, settlement in existing building, angle of distortion in existing building and evidence of open pit face failure.
- Training of a Soft Computing Method for prediction of maximum depth (V) to which an unsupported foundation pit for a new structure can be excavated and at what minimum safe horizontal distance (H) from an existing building can this pit be excavated.
- Compilation of outputs from modelling in PLAXIS and Machine Learning Model in the form of design charts to serve as guide for excavation practice.

1.4 Significance and Relevance of the Research

The rapid urbanization is leading to the need of advancement in efficient construction and design techniques. During the commencement of new construction project in conglomerated urban centers, the protection of neighboring structures is essential. The output will help determine safety of adjacent buildings against unsupported excavations. The output model and design charts will save time consumed in conventional FEM modelling and Limit Equilibrium Methods for determining safe parameters for open pit excavations. The machine learning model can evolve over time to accommodate new data to increase prediction accuracy.

1.5 Areas of Application

The prediction model from the proposed study is applicable to the construction industry involved in excavations for foundations of residential and low-rise commercial buildings constructed on soft homogenous soils with no encounter of ground water table.

CHAPTER 2

LITERATURE REVIEW

2.1 Introduction

Buildings and residential units are damaged due to excavation activities carried out in close vicinity to lay foundations of new structures to accommodate the ever-increasing development in urbanized areas. Excavation for a new building foundation can lead to structural damage in the nearby existing building by inducing settlements in the foundations which in turn induce structural damage in buildings such as cracks, jammed doors and windows and architectural damage. The damages are more pronounced when unsupported excavations are carried out near existing structures. Since there are no protective measures involved, the settlement and pit face failure can occur with no warning and can cause not only irreparable damage to structures but a loss of human life as well. In developing nations like Pakistan, unsupported excavations are very common in the construction of residential units. The structural, aesthetical and serviceability damages require costly repairs and expensive preventive measures to stop further damage. Therefore, a guide to determine the safe depth of unsupported excavation and lateral distance from the existing structures is crucial. It is necessary to determine the lateral range of excavation impact zone (Dmochowski & Szolomicki, 2021). This research is aimed to reduce damage to adjacent buildings during foundation construction in densely populated urban regions where unsupported excavations are resorted to by providing aids for unsupported excavation practices.

2.2 Unsupported Excavations

In open-cut or unsupported excavations, there is no support provided to the walls of the pit. Precautions are adopted to minimize horizontal and vertical displacements in the soil mass and structures built on it. Excavations with deep vertical cuts pose a threat to the stability of the existing nearby structures. These failures can be mitigated with excavation support systems such as bracing, shoring, retaining walls, secant piling, etc. In developing countries, lack of budget, facilities, and expertise play a role in the lack of use of these technological advancements (Hussain et al., 2019,Sivakrishna et al., 2020). The last resort

is open-pit excavations. The pit construction leads to a rebound phenomenon, causing the foundation pit to be unstable which poses a threat to neighboring structures (Ngoc et al., 2020).

2.3 Damage to buildings near excavations

The instability of existing buildings due to adjacent excavation can arise due to three reasons.

1) Differential settlement of foundation due to pit excavations (Zhang, 2020),

2) Distortion of foundation (Burland & Wroth, 1974) and

3) Failure of excavation pit face similar to slope stability failures (Wang et al., 2020, Hu & Ma, 2018).
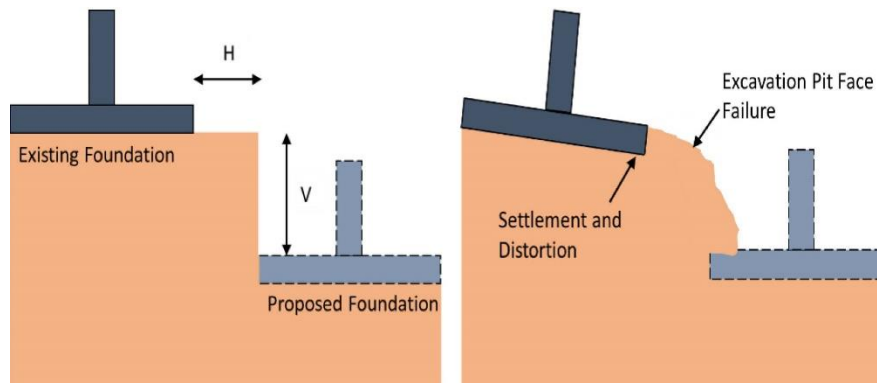
Figure 2.1 Damage to Adjacent Building due to Open Pit Excavation

2.4 Excavation Standards

There exist a few excavation standards for open pits such as: Bowles 1997, OSHA – US Department of Labor, Canadian Centre for Occupational Health and Safety – CCOHS, and Capital Development Authority (CDA) – Islamabad.

2.4.1 Bowles 1997

If an unsupported excavation is made near a foundation, the exposed vertical surface can rupture and slide due to the removal of lateral support. This is called bulging. Differential settlement and angular distortion can be induced because of soil movement. A safe depth (z) of excavation can be computed by the following formula with the consideration of pressure from existing footing:

$$\sigma_1 \approx \gamma z + q_0 \qquad \text{2.1}$$

$$\sigma_3 = 0 = \sigma_1 K - 2c\sqrt{K} = \gamma z K + q_0 K - 2c\sqrt{K} \qquad \text{2.2}$$

$$z = \frac{2c}{(\text{SF})\gamma\sqrt{K}} = \frac{q0}{(\text{SF})\gamma} \qquad \text{2.3}$$

where, σ_1 is vertical load, σ_3 is lateral load, γ is soil density, z is depth of excavation, K is co-efficient of lateral earth pressure, c is cohesion, q_o is pressure from existing footing and SF is factor of safety (Bowles, 1997). However, the safe distance of open pit excavation from an existing foundation cannot be determined with certainty.

2.4.2   OSHA – US Department of Labor

The Occupational Safety and Health Administration's (OSHA) Excavation standards, 29 Code of Federal Regulations (CFR) Part 1926, Subpart P, contains requirements for excavation and trenching operations (U.S Department of Labor, 2015). The aim of the standards is to prevent risk of cave-in and worker injuries and fatalities. The code categorizes soils into four types. Stable Rock is any material which when excavated retains intact and can be excavated with vertical sides. Type A soil is cohesive soil with an unconfined strength of 144 kPa. Type B soil is cohesive soil with an unconfined strength greater than 48 kPa but less than 144 kPa and granular cohesionless soils. Type C soil is cohesive soil with an unconfined compressive strength of 48 kPa or less, granular soils (including gravel, sand, and loamy sand), submerged soil or soil from which water is freely seeping, submerged rock that is not stable, or material in a slope. The maximum allowable unsupported excavation depth is 20 ft (6.09m). The allowable slopes are shown in table 2.1. The code provides guidelines for excavation depth and slope angles for unsupported excavations in various soils. However, adjacent foundations and safe distance from adjacent foundation are not considered. Moreover, the damage assessment metric is only the possibility of a cave-in.

Table 2.1 Soil Classification in OSHA

Soil type	Height: Depth ratio	Slope angle
Stable Rock	Vertical	90°
Type A	¾:1	53°
Type B	1:1	45°
Type C	1½:1	34°
Type A(short-term)	½:1	63°

2.4.3 Canadian Centre for Occupational Health and Safety – CCOHS

Standard number 1926.651 subpart P addresses excavations. The standard endorses the same guidelines as OSHA. However, CCOHS recommends caution against cave-in in trenches of depths 1.2 meters (4 feet) or more in soils.

2.4.4 Capital Development Authority (CDA) – Islamabad

If two buildings are on the same plot, the distance them between as recommended by CDA byelaws should be as follows:

1. If buildings overlap each other up to 12 ft, the minimum distance between them should be 6 ft.

2. If buildings overlap each other more than 12 ft, the minimum distance between them should be 10 ft.

The minimum distance between two residential units depending on their plot size is provided under "Zoning Bulk and Height Regulations for Residential Plots" in CDA byelaws (*Islamabad Residential Sector Zoning-Building Control Regulations*, 2005). However, these distances are recommended for illumination and ventilation purposes. The building byelaws do not consider the depth of pit excavations and their influence on adjacent buildings.

The summary of these standards and recommendations is shown in table 2.2.

Table 2.2 Summary of Recommendations and Standards for Un-supported Excavations

Sr. No	Researcher/Standard	Proposed Guidelines	Damage Evaluation Criteria	Soil Type	Deficiencies
1	(Bowles, 1996)	Safe excavation depth is proposed: $z=\dfrac{2c}{(SF)\gamma\sqrt{K}}=\dfrac{q0}{(SF)\gamma}$	• Settlement • Distortion	Applicable to all soil types.	No guidelines to determine safe distance from adjacent foundation
2	(U.S Department of Labor, 2015)	Excavation depth and slope angles for unsupported excavations in various soils	Cave-ins	Soils categorized as: stable rock, type A,B and C.	• No guidelines to determine safe distance from adjacent foundation • Foundation settlement and distortion not considered
3	Canadian Centre for Occupational Health and Safety	Excavation depth and slope angles for unsupported excavations in various soils Imposes a limitation of 1.2 m in soils.	Cave-ins	Soils categorized as: stable rock, type A,B and C.	• No guidelines to determine safe distance from adjacent foundation • Foundation settlement and distortion not considered
4	Capital Development Authority (CDA) – Islamabad	The minimum distance between two residential units depending on their plot. These are open spaces for illumination and ventilation purposes.	None	Not Mentioned	• No guidelines to determine safe distance from adjacent foundation • Foundation settlement and distortion not considered

2.5 Previous Studies

Bakr, 2019 proposed that in absence of adjacent buildings in stiff and medium stiff soils, an unsupported excavation of 9m can be made. In case of adjacent buildings, a distance must be left depending on the load. Irfan et al., 2013 proposed a regression model to estimate the factor of safety for unsupported excavations in Lahore, Pakistan. It was established that the clay layer cohesion was the most dominant contributor to safety factor. The adjacent buildings were not on site to be considered. Aljorany & Al-qaisee, 2018 observed ground surface settlements due to unsupported excavations in Iraq at varying horizontal distances. The adjacent buildings were not on site to be considered. Shahnazari et al., 2018 evaluated critical depth of excavation for clay numerically and physically. However adjacent buildings and horizontal distance were not considered. Richard et al., 2016 provided estimates for height of unsupported excavations in unsaturated sands. The height depends on shear strength and matric suction. Brennan et al., 2020 estimated the critical height of unsupported excavation to be 0.7 meters in sands. The studies are summarized in table 2.3.

Table 2.3 Summary of Previous Studies

Researcher	Soil Type		Adjacent Buildings Considered	Safe Distance Limits	Safe Depth Limits
	Clay	Sand			
(Bakr, 2019)	✓ (Stiff)		✓	✓	✓
(Irfan et al., 2013)	✓		✗	✗	✓
(Aljorany & Al-qaisee, 2018)	✓		✗	✗	✓
(Richard et al., 2016)		✓	✗	✗	✓
(Brennan et al., 2020)		✓	✗	✗	✓
(Shahnazari et al., 2018)	✓		✗	✗	✓

✗ *Parameter considered*   ✓ *Parameter not considered*

2.6 Building Deformation Identification

Crack patterns in structures testify differential settlements which have occurred or are still in progress (Alessandri et al., 2015). Cracks produced by foundation movement are concentrated at points of maximum structural distortion (Bonshor et al., 1998). Uneven settlement of foundations leads to cracks in superstructures. The cracks are vertical in walls and diagonal near openings. The cracks are usually tapered, wider at the top and narrower at the bottom of the walls (Grimm, 1988, Ercio et al., 2006). Excavation adjacent to existing structures induces hogging in the foundations. In such cases the cracking initiates from top of the walls and proceeds to the bottom (Giardina, 2013). If the foundation is rigid, a rigid rotation (tilt) can also occur (Dalgic et al., 2018). The source of settlement can be pointed out by making a straight line over the crack. A perpendicular arrow drawn on the straight line indicates the location of settlement as shown in figure 2.4.
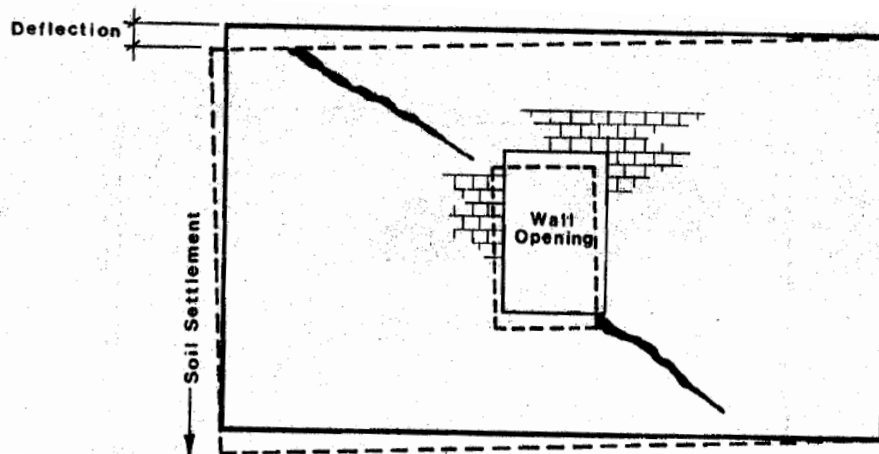
Figure 2.2 Crack pattern in wall with opening. (Grimm, 1988)
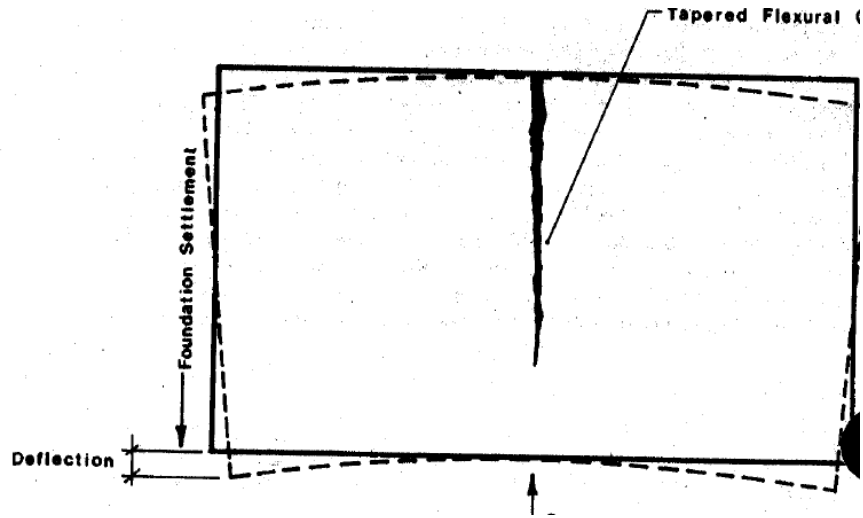
Figure 2.3 Crack Pattern in wall without openings. (Grimm, 1988)
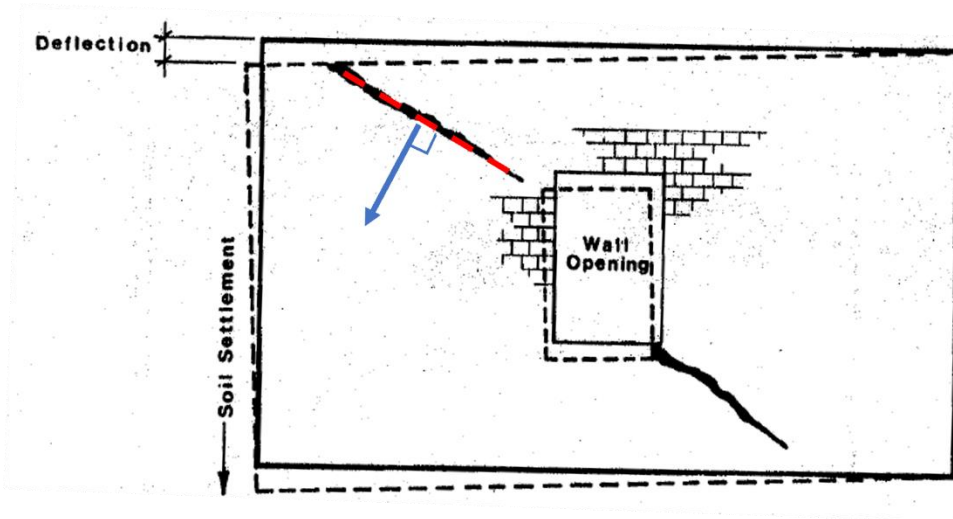
Figure 2.4 Indication of Settlement Source form Crack Orientation

2.7   Settlement Measurement

Building damage can be assessed from measurement of deformation in structural elements of a building. One of the most useful techniques is the interior levelling of the building. The process is usually applied to maintain gradient of slopes of roofs and floors for drainage. The same procedure can be used to determine levels at different locations of a floor or slabs (Ruiz-Jaramillo et al., 2016). In the rise and fall method of levelling, an engineering level and a levelling staff is employed. The elevation difference is calculated

by taking the difference between the forward staff reading and preceding staff reading. A rise is said to have occurred if the forward reading is smaller than the preceding reading and fall is said to have occurred otherwise (Mehmood et al., 2018,Ruiz-Jaramillo et al., 2016). A schematic illustration is shown in figure 2.5.
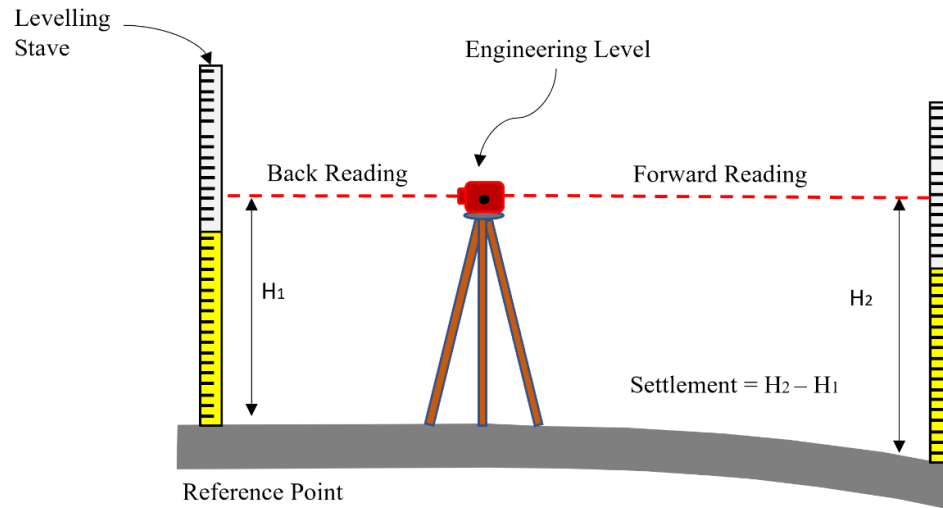
Figure 2.5 Settlement Observation

2.8 Safe Limits of Deformation (settlement, distortion, and pit face failure)

The following conditions maybe set to categorize the excavated pit as safe:

1. For existing foundation during excavation (Fig. 2.1):

   i.   Maximum Differential Settlement at points A and B < 25mm
   ii.   Maximum Distortion Angle (b) $< 1/500$

The above were extracted from European Committee for Standardization on Differential Settlement Parameters (Bond et al., 2013).

2. For Excavation Pit:

   i.   No vertical face failure (Mohr Columb Criteria)
   ii.   There is no excavation support system

2.9 Machine Learning

Due to complexity of geotechnical materials and calculation procedures, researchers tend to replace tedious calculations with soft computing skills to provide solutions for geotechnical engineering problems. Many uncertainties are associated with geotechnical problems and various parameters cannot be determined directly. This has led to the rapid popularity of Machine Learning. Machine Learning algorithms can recognize potential relationships between different parameters without any prior assumptions or training. Artificial Intelligence (AI) is basically intelligent programs which can imitate humans in decision making. Machine Learning is a subset of AI (Zhang et al., 2021). The most significant use of machine learning is in instances when there are many input and output parameters under consideration and no numerical or empirical equations exist to establish relations between them.

2.10 Types of Machine Learning (Supervised and Unsupervised)

There are two major types of machine-learning i.e., supervised, and unsupervised. In supervised machine learning a function maps an input to an output based on example input-output pairs. The machine learning needs external assistance. The data is divided into training and testing groups. The training data has both inputs and outputs, and the algorithm learns to predict outputs based on inputs. The remaining data set is used to test the trained algorithm. It only provides the input to the trained model and determines if the predicted output matches the actual output (Batta, 2020,Singh et al., 2016). The workflow is shown in figure 2.6. In contrast, unsupervised learning uses algorithms to analyze and cluster datasets. The algorithms discover the patterns on their own without human intervention. The algorithms are not provided with input-output examples, rather the algorithm devises relations on its own between different input and output parameters.
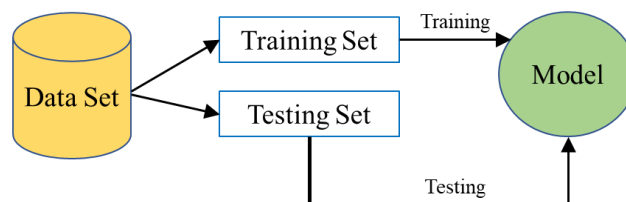
Figure 2.6 Supervised Machine Learning

2.11 Supervised Machine Learning Algorithms

2.11.1 Logistic Regression

This technique is applied when the output data is dichotomous i.e., it has only two possible output values. It is specifically used for data classification. It assumes that the data is free of any missing values and the inputs are independent of each other. Logistic regression is an extension of linear regression. Linear regression cannot be employed if the dependent variable is of dichotomous nature. Logistic regression is employed to predict relationship between the input and output variables when the output values are binary. The logistic distribution is an S-shaped distribution function which is similar to standard normal distribution and the estimated probabilities lie between 1 and 0. However, to calculate the probability, we need to calculate Z. Z is a linear function of the input variables. The natural log of the odds is called "logit" function. Logit applied to Z determines the probability P.

$$Z \ = \ ln \ \frac{P}{1-P} \qquad\qquad 2.4$$

2.11.2 Decision Trees and Random Forests

Decision trees are a good classification tool. The decision tree builds algorithms on if-then rules and expands like the branches of a tree. The split at each node is based on the input parameter which provides maximum information gain. The process goes on with breaking down the data into smaller structures with incremental decisions until the termination point. The final structure looks like a tree with nodes and leaves. New data is classified from a root node to a leaf node where a test is performed for classification. The algorithm can handle binary and multiple classification problems. A random forest is an ensemble of decision trees (Aly, 2005,Kohestani et al., 2017). A decision tree is shown in figure 2.7.
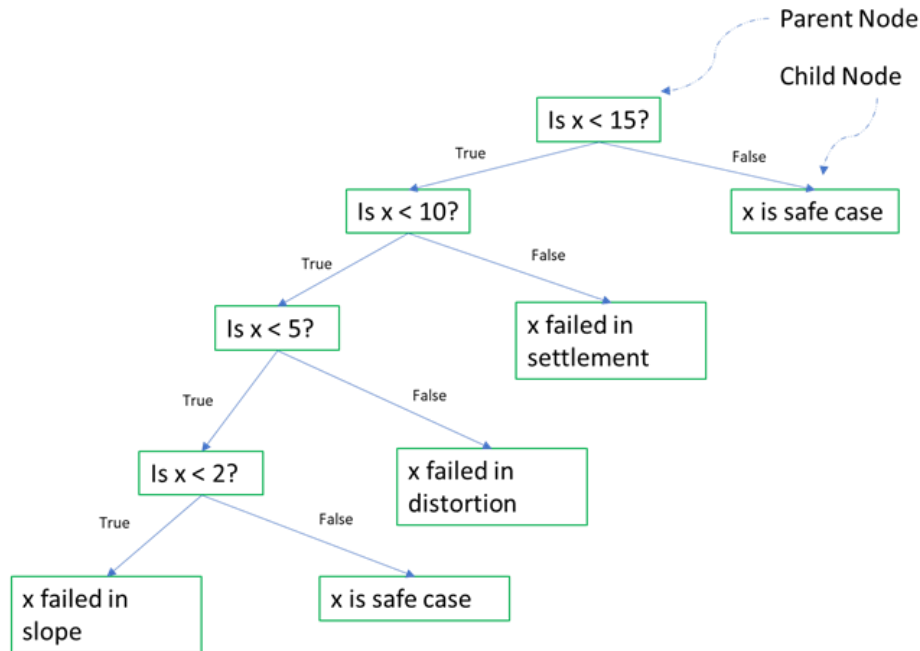
Figure 2.7 Decision Tree

2.11.3 Artificial Neural Networks or Multilayer Perceptron

A neural network is composed of neurons which apply mathematical functions to the input to produce an output. There can be several layers of neurons between the input and the output layers. Each neuron may take the output of the neurons in the previous layers as its input. There are many classes of neural networks, the most common is Multi-Layer Perceptron. These consist of one input layer and one output layer and one or several hidden layers consisting of the neurons.

Any value multiplied with input or output of a neuron is called a weight while anything added is called bias. A neural network learns to adjust weights and biases to minimize the error between predicted and desired output (Commend et al., 2019,S. B. Kotsiantis, 2007). Ultimately all outputs are summed using an activation function e.g., hyperbolic function, sigmoid function, ReLu etc. Figure 2.8 shows the architecture of a Neural Network.
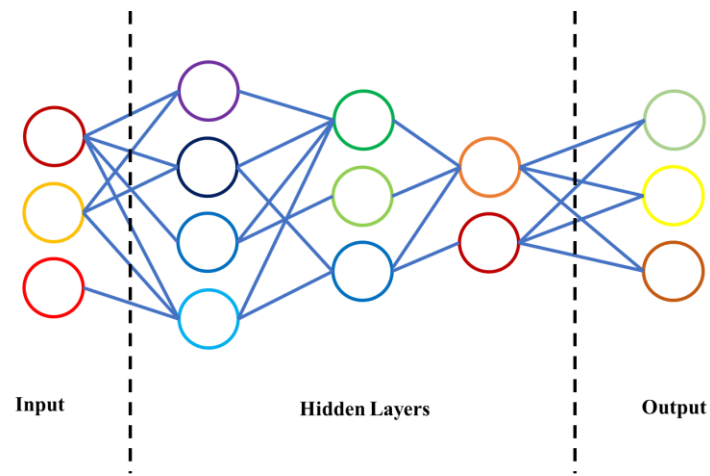
Figure 2.8 Neural Network Architecture

2.11.4 Support Vector Machines

Support vector machines are robust classification tools. These not only support binary classification, but extensions can handle multiclass classifications as well. The support vector machine represents training data points in space separated into categories with as wide spaces between as possible. This is called the idea of maximizing the margin. The new points are added to the categories in the space where they belong. Support Vector Machines are particularly useful with high dimensional data (Cortes & Vladimir, 1995).

2.11.5 K-nearest neighbor

K-nearest neighbor assumes that similar things exist in proximity. It can be explained by a simple rule that to classify an unknown point, choose the class nearest in the training data set based on a distance metric. It functions by calculating the distance between a query point and the examples in the training data. It then selects the specified number of examples closest to the query then averages the output values of those closest neighbors to predict the required output for the query under consideration (Bay, 1999).

2.11.6 Gene Expression Programming

Gene Expression Programming (GEP) is another type of AI that is based on neural and regression techniques. GP has the ability to produce simple expressions. The output is characterized by simple mathematical equations (Javed et al., 2020).

2.12 Machine Learning with Scarce Data

Although machine learning algorithms require large amount of data for training and testing (Ouyang et al., 2021), there are examples where researchers employed small data sets to train machine learning models (Kohestani et al., 2017,Javed et al., 2020,Mahamat et al., 2021,Sameen et al., 2019,Dabbaghi et al., 2021). Small datasets are not ideal for machine learning model training but in instances when there are a number of input and output parameters, a relation can only be established with machine learning models.

2.13 Sensitivity Analysis

Sensitivity analysis allows the identification of parameters that have the most effect on the output. MLP model has the capacity to predict output variables but the mechanism which occurs within the network is often ignored. Knowledge of contribution of each variable is important. Garson (Garson, 1991) proposed a method to determine the influence of each variable in the MLP model. Consider a neural network has the network architecture as m x n x 1, where m is input nodes, n is hidden nodes and 1 is output node. The procedure is as follows:

1. Determine a row vector, M (1 x n), for the interconnection weights between the hidden nodes (n) and the output nodes.
2. Arrange a m x n matrix, W, for the interconnection weights between the input layer nodes (m) and the hidden layer nodes (n).
3. Calculate the row vector, R=MW^T.
4. Determine the relative importance in percentile using equation 2.5.

$$RI_i = \frac{|r_i|}{\sum_{i=1}^{m}|r_i|} x100\%, \quad i = 1\ to\ m \qquad 2.5$$

The higher the value of the relative index, the higher the importance of that input variable (Lee & Hsiung, 2009). Local sensitivity analysis can also be applied to the models. It evaluates changes in output models with variations in the input parameters. The input parameters are typically changed one at a time in very small intervals (e.g., 10% folds). The effect of individual parameter changes is determined using local sensitivity indices (Hamby, 1994,Wolkenhauer et al., 2008).

2.14 PLAXIS

PLAXIS is a finite element analysis computer program which is used for deformation and stability analysis of multiple construction stages for various geotechnical engineering applications. Pre-defined structural elements and CAD like environment allow fast and efficient model generation and simulation. Complex finite element models can be generated with simple inputs and outputs presenting detailed computational results. PLAXIS recognizes clusters inherently. Clusters are enclosed areas made up of points and lines in which the material properties are homogenous. After creation of geometric model, FEM mesh can be generated in the clusters. During meshing the clusters are divided into triangular segments. 15 node elements are more accurate but time consuming as compared to 6 node elements. After the creation of geometry, different types of loading conditions can be applied under a number of construction stages. Moreover, the loading conditions causing a known amount of deformation can also be determined.

CHAPTER 3

METHODOLOGY

3.1 General

The city of Mirpur Azad Kashmir, Pakistan was selected for the study. The first step was to identify sites where unsupported excavations were being done next to adjacent structures. This was followed by data collection. The data collected for the study included building parameters which were building dimensions, building load, settlement measurement and pit face failure identification. The depth of the excavation pit and distance from the adjacent building were also determined. Soil parameters were also determined which included in-situ soil density and moisture content measurement. The soil was classified based on USCS classification in the lab. Unconfined compression tests were performed to determine the cohesion and elastic modulus of the soil. Three machine learning models were trained i.e., Multi-layer Perceptron, Gene Expression Programming and Decision Tree. Sensitivity analysis proposed by Garson and local sensitivity analysis were applied on the models to identify the influential parameters to reduce the number of inputs for modelling in PLAXIS. Design charts were made from results complied from PLAXIS. The inputs for PLAXIS were also provided to the machine learning model. Finally, the design charts were validated against case studies. The methodology is summarized in figure 3.1.
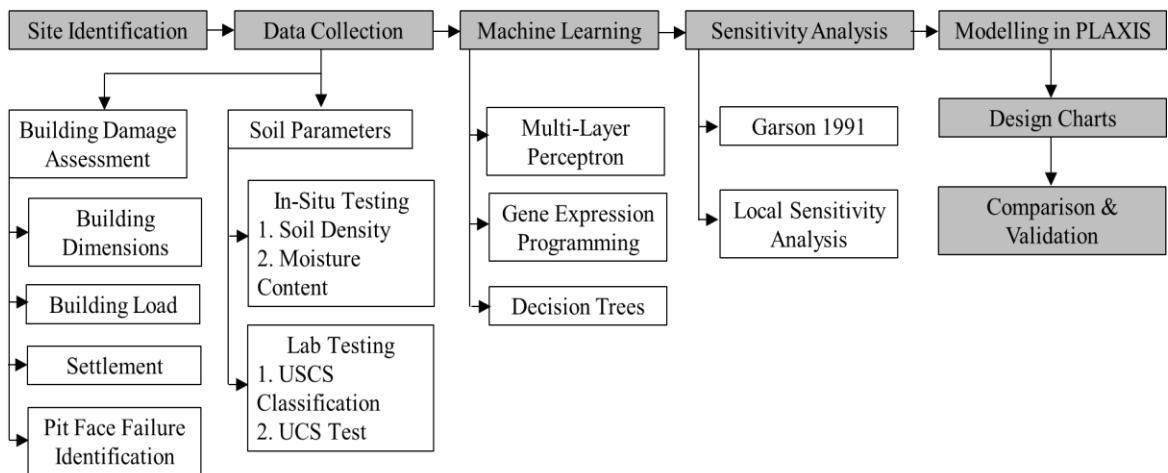
Figure 3.1 Methodology

3.2 Area of Study and Site Identification

The city of Mirpur Azad Kashmir was selected for the study. The city lies at 135 km southeast of the capital city Islamabad. The city was an ideal site for observing excavation and construction related activities. Mirpur lies near Mangla reservoir. In 2004 due to excessive sedimentation, the dam was raised by 9 meters and the construction was completed in 2009. Mirpur was one of three towns directly affected by the upraising. The effected population was resettled and compensated in New Mirpur City. Many residents had to abandon their homes and buildings and construct new ones in New Mirpur City and in areas unaffected by the upraising. This led to an exponential increase in building construction in the region. The number of newly constructed residential buildings was especially large. This led to ideal conditions to observe building damages in existing buildings in the vicinity of which unsupported excavations were being done to construct foundation for new buildings. Reconnaissance survey was done of Mirpur city and sites were located where excavation was being carried out near buildings. Most of the excavations were being done next to residential units. The sites identified included the areas of Sector F2, Ban Khurman, Y-Cross, Sector D4, Sector F4, Sector F3 and New City.
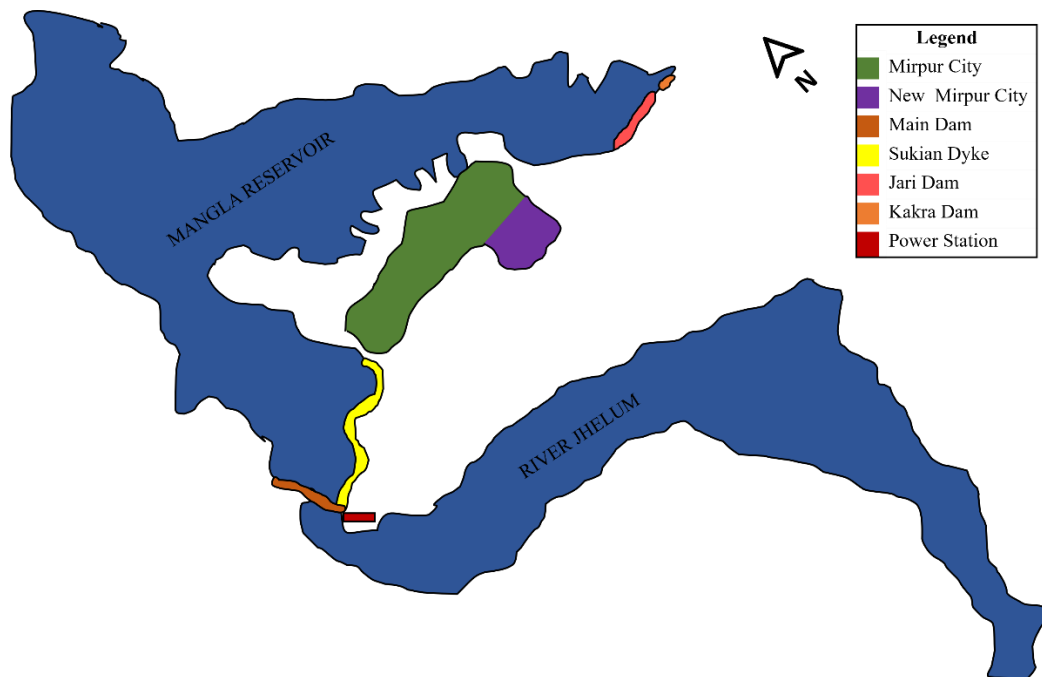

Figure 3.2 Map of Mirpur City

3.3 Data Collection

From the identified sites, building damage assessment was done and soil samples were taken for lab testing. In-situ soil tests were also performed. The survey form is attached as Annex-A. The details are given below:

3.3.1 Building Damage Assessment

The building damage assessment comprised of: building dimension measurement, building load calculation, settlement measurement, pit face failure identification, dimensions of unsupported excavation.

The dimensions of unsupported excavations were measured with a measuring tape. The depth of the unsupported excavation and the lateral distance of the unsupported excavation from the existing building was recorded. The dimensions of the buildings were also measured using an ordinary measuring tape. The units of measurement were in meters. The load was calculated using the building covered area plan and average unit weights of the construction materials. The average live load selected was 1.5 kN/m^2. Unit weights of construction materials and dimensions of building components are given in tables 3.1 and 3.2 respectively.

Figure 3.3 Measuring Tape

Table 3.1 Unit Weights of Construction Materials (Zain et al., 2019,Mohafezatkar Sereshkeh & Jamshidi Chenari, 2017)

Material	Average Unit Weight kN/m^3	Selected Unit Weight kN/m^3
Concrete	22.7-23.5	22.7
Masonry (Bricks)	15.7-20.4	15.7

Table 3.2 Typical Dimensions of Building Components

Component	Dimensions
Slab	150 mm thick
Wall	2.7 m high
	200 mm thick

The settlement was measured using the fall and rise method of levelling using an Engineering Level and a Levelling Staff. In the rise and fall method, the elevation difference is calculated by taking the difference between the forward staff reading and preceding staff reading. A rise is said to have occurred if the forward reading is smaller than the preceding reading and fall is said to have occurred otherwise(Mehmood et al., 2018)(Ruiz-Jaramillo et al., 2016). During observation, the point near the excavation was taken as forward point and the point farthest away from the excavation in the building was taken as the reference point. To avoid errors due to local floor sagging, material failure or wear, multiple readings were taken. A schematic illustration is shown in figure 3.4.
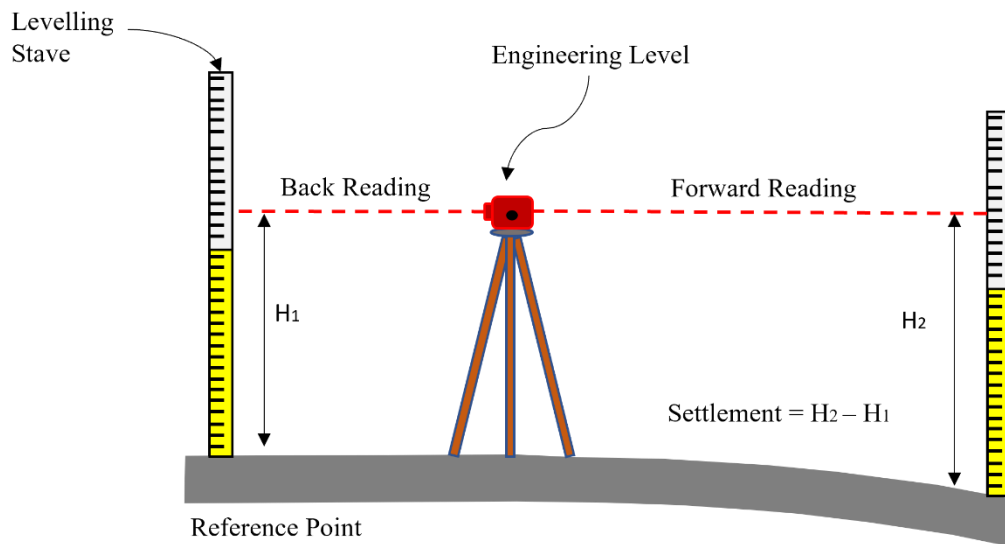

Figure 3.4 Settlement Observation

A few qualitative observations were also made during the survey which included observations for cracks in walls and floor and jamming of doors and windows. The pit face

failure identification was a judgment-based observation. It was clearly evident at locations where the slope failures had occurred. The displaced soils had moved entire structures built on them. Figures 3.5(a) and 3.6(a) show unsupported excavations near residential units and figures 3.5(b) and 3.6(b) show the resulting architectural damage caused due to settlement in the floor and wall respectively. Figures 3.7(a) and 3.7(b) show pit face failures due to unsupported excavations.

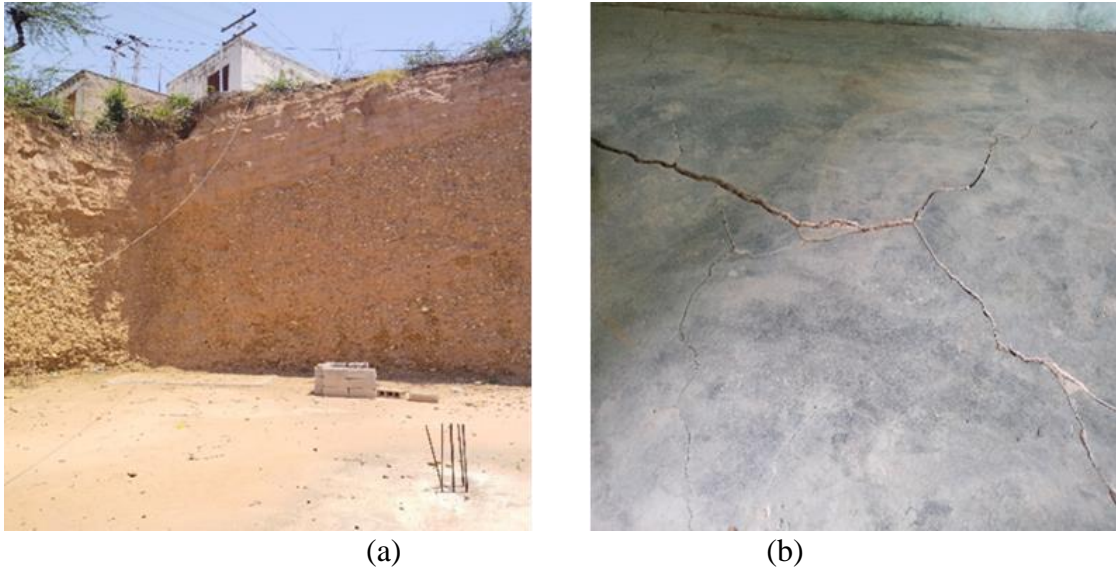(a)   (b)

Figure 3.5 Unsupported excavation near a residential unit and induced
settlement damage in Sector F-2

(a)   (b)

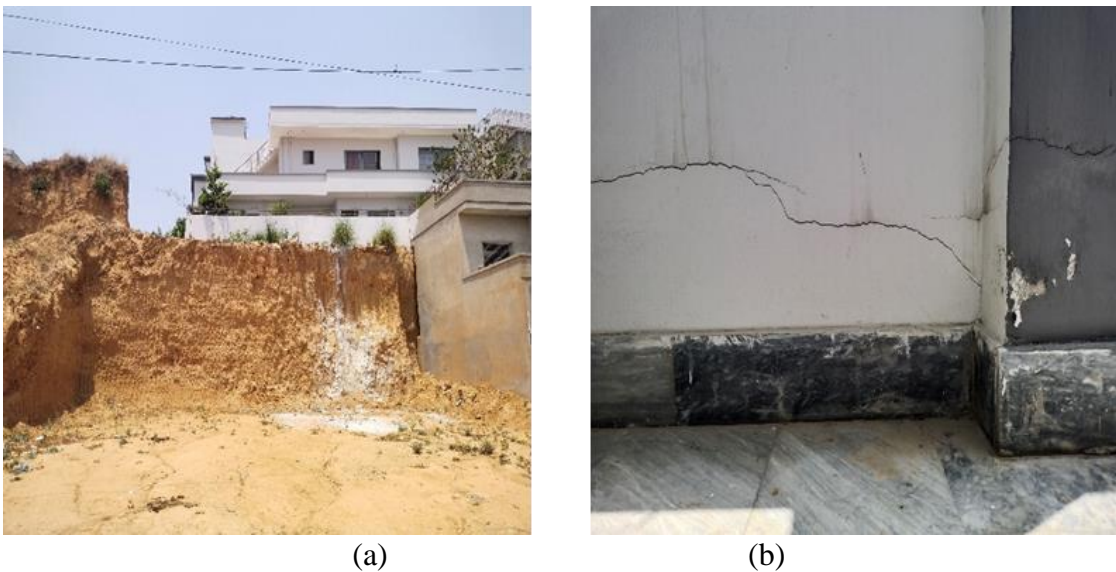Figure 3.6 Unsupported excavation near a residential unit and induced

architectural damage in Sector F-4

<center>(a)   (b)</center>

<center>Figure 3.7 Pit-face failures due to unsupported excavations in Y-cross</center>

<center>and Sector F-3</center>

3.3.2   Soil Parameters

In-situ tests were performed to determine density and moisture content. Laboratory tests were performed to determine USCS soil type, cohesion and elastic modulus of the soil.

Sand cone replacement method was used to determine the in-situ density of soil (ASTM D1556-00, 2016). A small hole was dug in the soil and the excavated soil is weighed. The excavated hole was filled with sand to determine its volume. In-situ density was determined by dividing the mass of the excavated soil with the volume of the hole. The dry density of the soil can also be determined by first determining the moisture content of the soil. The soil excavated during in-situ density measurement was stored in plastic bags for transportation to laboratory for testing.

The moisture content in the field was determined by employing Speedy Moisture Test (ASTM D4944-18, 2018).The moist soil specimen was placed in the testing apparatus with two steel balls and calcium carbide. The instrument was closed off tightly and shaken vigorously. Acetylene gas was produced proportional to the amount of water present in the soil sample. The reading given by the pressure gauge is the amount of moisture present in the sample in percentage.

Figure 3.8 In situ soil density measurement

Figure 3.9 In situ moisture content measurement

Sieve analysis (ASTM D6913, 2021), Hydrometer analysis (ASTM D7928, 2021) and Atterberg's Limits (ASTM D4318, 2018) were used to classify soil based on Unified Soil Classification System USCS (ASTM D2487, 2020).

USCS identifies three categories of soil types i.e., coarse-grained, fine-grained and highly organic soils. There are 15 sub-divisions of these categories. The soil is categorized based on visual observations and laboratory tests.

Sieve analysis is done to determine particle size distribution of a soil sample. The sample must be oven-dried and pulverized first. The soil is placed in the sieve set and it is shaken. Mass retained on each sieve is determined. The results are graphically represented as a gradation curve.

Hydrometer analysis is used to determine the particle size distribution of material finer than No. 200 sieve (75-µm). The specimen is mixed with a dispersing agent and water. The resulting slurry is placed in a test cylinder and additional water is added. Readings are taken at specific time intervals with a hydrometer. Temperature is also noted to apply corrections.

Atterberg's Limits are liquid limit and plastic limit. The material passing through sieve number 40 (425-µm) is used for the tests. Casagrande's apparatus is used to determine the liquid limit. The liquid limit is determined by performing trials. In each trial the amount of water content is changed. The conventional practice is to move from dry to wet state. In each trial the sample is spread in the brass cup and divided into two segments using a grooving tool. The blows are counted until the two separated segments meet by about half an inch. The moisture corresponding to 25 blows is the liquid limit of the soil.

The plastic limit corresponds to the moisture content where the soil can no longer be rolled into threads of 1/8 inch diameter without crumbling. The plasticity index is the difference between liquid limit and plastic limit.

ASTM D2166 was employed to determine the unconfined compressive strength of the soil specimens (ASTM D2166, 2016). The soil sample is loaded axially at an axial strain rate between 0.5 to 2% per minute. Axial deformation, axial load and elapsed time are noted. The half of unconfined compressive strength is undrained shear strength of the soil. The

modulus of elasticity was determined from the stress-strain curve. The following relationship is used:

$$E_{u50} = \frac{\partial \sigma}{\partial \varepsilon_{50}}$$

3.1

where, E_{u50} is modulus of elasticity, $\partial \sigma$ is change in vertical stress and $\partial \varepsilon_{50}$ is strain at 50% of peak strength value.

Figure 3.10 Sample Collection

Figure 3.11 Oven Drying

Figure 3.12 Pulverization

Figure 3.13 Hydrometer test
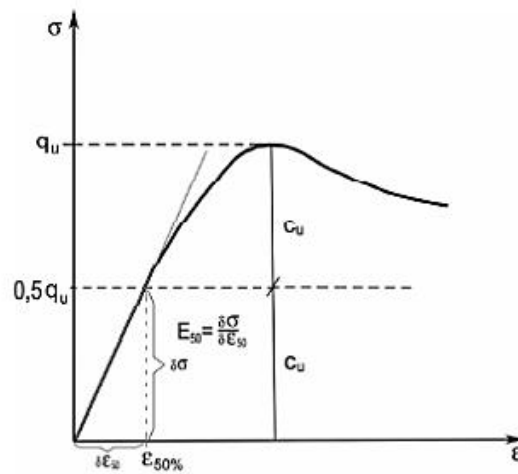

Figure 3.14 Unconfined Compression Test

Figure 3.15 Derivation of Modulus of Elasticity (Strózyk &
Tankiewicz, 2016)

3.4   Soil Classification and Categorization

The soil can be categorized as soft, medium or stiff based on the ranges of Young's Modulus (Truty, A., & Obrzud, 2011,Kézdi & Rétháti, 1974). The values are given in table 3.3.

Table 3.3 Typical Values of Young's Modulus (MPa)

USCS Type	Description	Very soft to soft	Medium	Stiff to very stiff	Hard
ML	Silts with slight plasticity	2.5 - 8	10 - 15	15 -40	40 - 80
ML, CL	Silts with low plasticity	1.5 - 6	6 -10	10 - 30	30 -60
CL	Clays with low-medium plasticity	0.5 - 5	5 -8	8 - 30	30 - 70
CH	Clays with high plasticity	0.35 - 4	4 -7	7 - 20	20 - 32
OL	Organic silts	-	0.5 -5	-	-
OH	Organic clays	-	0.5 -4	-	-

3.5   Machine Learning

The dataset collected from the field was trained in three machine learning algorithms i.e., Multi-layer Perceptron (MLP), Gene Expression Programming (GEP) and Decision Trees (DT). These machine learning algorithms were chosen because of their tendency to give good results with small data sets. 70% of the data was used to train the algorithms while 30% of it was used to test the models. The training and testing accuracies of the models were compared with each other to determine which model was most suitable for predicting if a selected combination of unsupported excavation depth and the lateral distance from an existing structure was safe or not. MLP and DT were trained in IBM SPSS whereas GEP was trained in Gene X Pro Tools.

3.6   Sensitivity Analysis

Out of the 7 input parameters, the most influential parameters were selected for the machine learning algorithms for creating design charts. The method proposed by Garson and local sensitivity analysis were applied to the MLP model. Garson 1991 method determines the

influence of each input variable in the MLP model based on associated weights and biases. The method has been explained in detail in section 2.13. Local sensitivity analysis evaluates changes in output with variations in the input parameters. The input parameters are typically changed one at a time in very small intervals (i.e., 10% folds). An average of ranking index from both methods was taken to determine the most and the least influential parameters.

3.7   Modelling in PLAXIS

To create design charts the uninfluential parameters were ignored, and the remaining parameters were varied in combinations within their maximum and minimum values. The modelling was done in PLAXIS. The model in figure 3.16 was constructed in PLAXIS v.8 software for each combination of selected input parameters. The pit was excavated in stages of one-meter intervals as shown. The load was applied to the foundation in the first stage. In the first one-meter excavation stage the displacements were set to zero so settlements in the foundation due to loading were not taken into account in the displacement caused by the excavation. The existing foundation shown in blue was horizontally displaced away from the edge of the pit at one-meter intervals. For each one-meter horizontal displacement, a staged excavation of one-meter intervals was modeled to 10-meter depth. The pit was excavated at one-meter intervals until one of the conditions quoted in section 2.8 had failed. Mohr-coulomb model was used to model soil behavior.

Figure 3.16 Staged Excavation at 1 m intervals

3.8 Design Charts

The most influential parameters from sensitivity analysis were taken as variables for modelling in PLAXIS while the remaining were taken as constants to reduce the number of modelling iterations. The most recurrent values of the variables were selected as inputs. Results from the modelling in PLAXIS were turned into graphical representation to allow users to select a suitable combination of unsupported excavation depth and the lateral distance from an existing structure for different soil parameters.

3.9 Verification and Comparison

The machine learning models and design charts from PLAXIS were verified from an external database and the models and charts were compared with each other to determine which had the most accuracy.

CHAPTER 4

RESULTS

4.1 Database

A database from precedents has been developed. The database consists of parameters from 44 case studied form Mirpur Azad Kashmir. The building parameters include dimensions and loads of existing buildings, distance of excavation pit from the existing building and depth of excavation pit. The soil parameters include soil type based on USCS classification, unit weight, cohesion and elastic modulus. The damage parameters include settlement of the building due to adjacent excavation and slope face failure. The database is attached as Annex B. The soils were predominantly low plastic clays. The elastic modulus of soils from the sites were determined experimentally. The values ranged from 0.08 to 1.88 MPa. As suggested by (Obrzud, 2010,Kézdi & Rétháti, 1974,Prat et al., 1995), soils having elastic modulus less than 2 MPa are regarded as soft soils. Hence, in the subsequent study, design models and charts are limited to soft soils only. For the soils, Mohr-Coulomb criteria was used for modelling in PLAXIS, and the internal angle of friction was taken as zero.

The targeted buildings were residential units. In residential units, the foundations of walls and columns are so close together that the foundations can be treated as mat foundations instead of isolated or strip foundations (Daud, 2012,Daud, 2012,Nangan et al., 2017). In this study, the further calculations have been made by considering mat foundations only. The following parameters were used for mat foundations in PLAXIS.

Table 4.1 Parameters for mat foundation in PLAXIS

Axial Stiffness (EA) (kN/m)	Bending Stiffness (EI) (kNm^2/m)	Foundation Thickness (D) (m)
5.000E+06	8500.000	0.143

4.2 Machine Learning Prediction Model

Three machine learning models were used in the study i.e., Decision Tree, Multi-Layer Perceptron (MLP) and Gene Expression Programming (GEP). The database was divided

into testing and training parts. Training dataset comprised of 70% while the testing dataset comprised of 30% of the database. Decision Tree and Multi-Layer Perceptron were modelled in IBM Statistics Software SPSS. For Gene Expression GeneXPro Tools 5.0 was employed. The three machine learning models were trained in such a way that if the building and soil parameters are entered along with the adjacent distance and desired depth of excavation pit, the models can predict if the combination of distance and depth is safe or not.

Out of the three machine learning algorithms, Multi-Layer Perceptron depicted the highest accuracy during the training and testing phase. The optimum results were obtained with two hidden layers and hyperbolic tangent as the activation function. The comparison of the different models is shown in the figure 4.1.
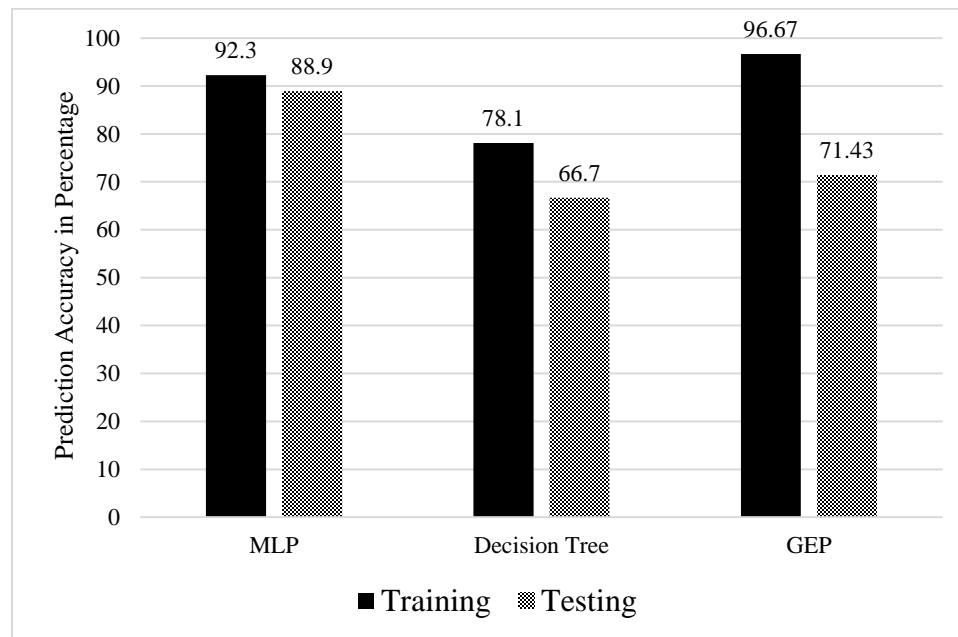
Figure 4.1 Comparison of Machine Learning Models

4.3 Sensitivity Analysis

Once an optimum machine learning model was obtained. Two types of sensitivity analysis were performed on it to determine the most sensitive input parameters i.e., Garson Method and 10% perturbation method. The Garson Method proposes influence of each input parameter based on connection weights within the neural network. For 10% perturbation method, case 20 was taken as base case and 10% variations were induced in one of the 7

parameters at a time while keeping the values of the rest constant. The resulting database was provided as a new input to the MLP model, and each case was determined as safe or unsafe. The influence of each parameter was recorded based on the observation that after how many 10% induced intervals of each parameter does the result of the model change from accurate to inaccurate. The results are shown in figure 4.2.
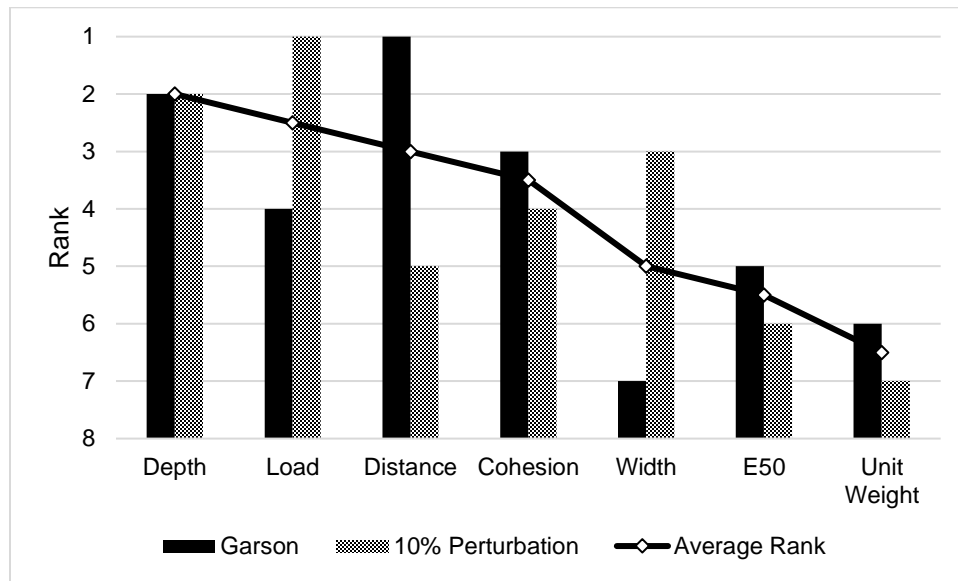

Figure 4.2 Ranking Index from Sensitivity Analysis

The parameters are ranked from 1 to 7, 1 being the most influential and 7 being the least. The average rank from the two methods was used in the study. Based on these results, elastic modulus and unit weight were the least influential parameters and were considered as constants during modelling in PLAXIS in the subsequent stage. Since all soils under consideration were soft soils, there was little variation in the values of these parameters which in turn resulted in no effect on the model.

4.4 PLAXIS Design Charts

The 5 most influential parameters i.e., cohesion, width, load, distance, and depth were used for modelling in PLAXIS. The most recurring values form the database were selected for modelling in PLAXIS. The values are listed in table 4.2. There were 60 combinations of the input values. The values of elastic modulus and unit weight were kept constant at 2 MPa and 17 kN/m^3. The combinations are enlisted in Annex-C. The results are shown in

figures 4.4 to 4.9. All combinations lying below the lines in the graphs are safe limits of distance and depth of excavation.

Table 4.2 Selected Values of Input Variables for Design Charts

Parameter	Values
Cohesion	5, 10 and 15 kPa
Width	7.5, 10, 13.5, 16 and 20 m
Load	10, 20, 30 and 40 kPa
Distance	0 to 10 m (1-meter intervals)
Depth	0 to 10 m (1-meter intervals)

4.5   MLP Model Based Design Charts

Although MLP model can itself provide predictions of safe combinations of distance and depth of excavation, but the combinations used in Annex-B were also provided as input to the MLP model to produce design charts comparable to PLAXIS design charts. The results are shown in figures 4.10 to 4.15. The combinations of cases which lie below the lines in the graphs are safe while the combinations which lie above are unsafe. The illustration of a design chart is shown in figure 4.3.
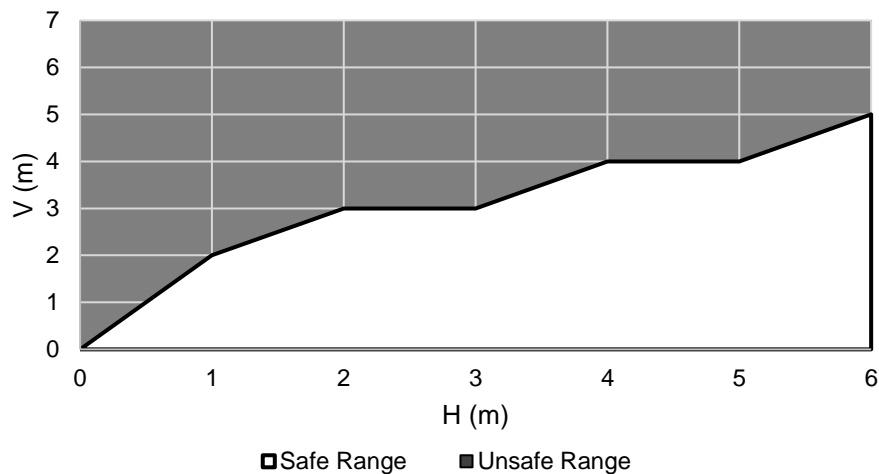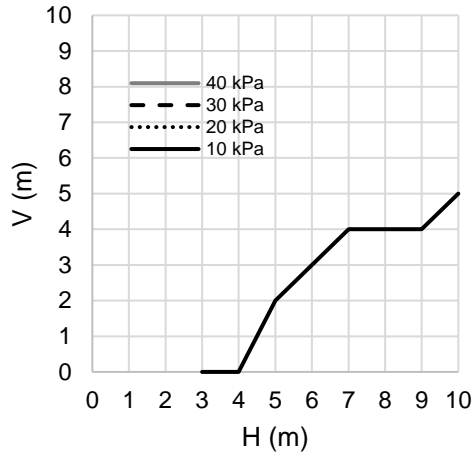

Figure 4.3 Illustration on use of design charts

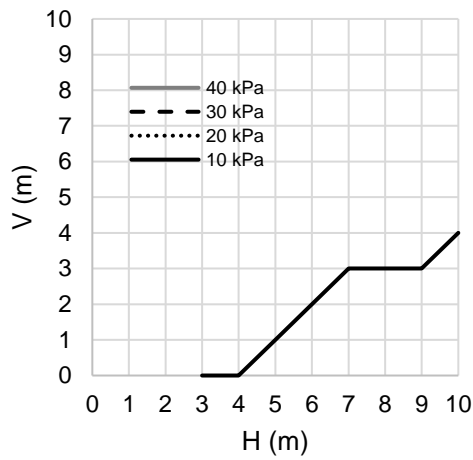The use of design charts is shown below:

1.   Select the group of charts with the cohesion of the soil.

2.   Select the chart with the desired foundation width.

3.   Select the load on the foundation.

4.   Any combination of depth of unsupported excavation (V) and lateral distance (H) which lies below the black line is safe and vice versa.
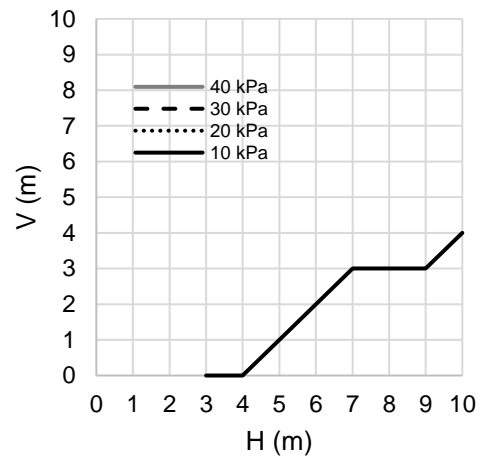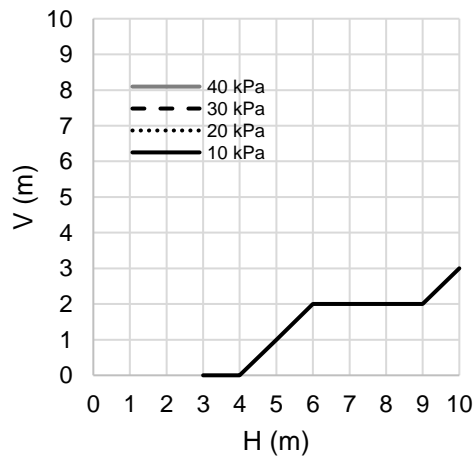
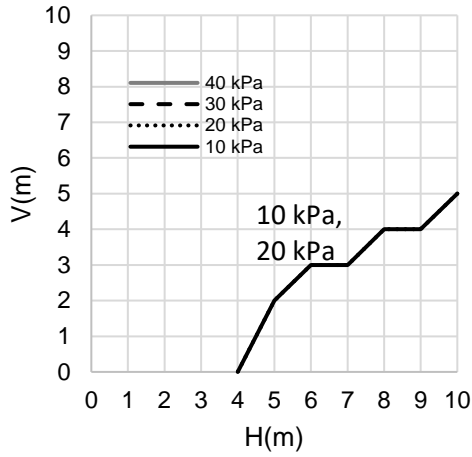(a) Width 7.5m
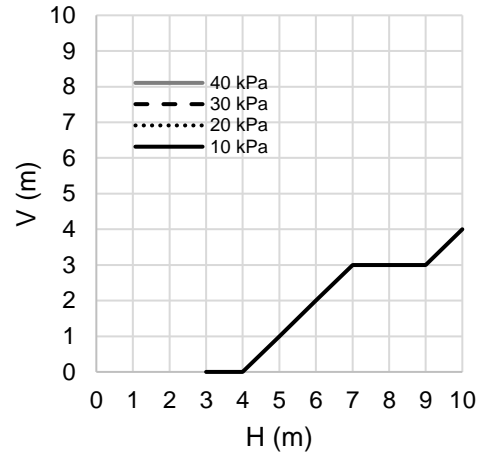
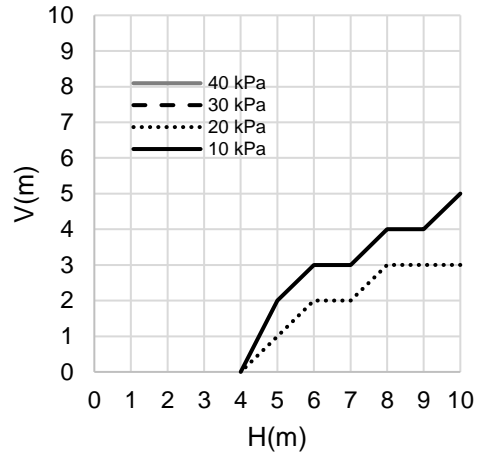(b) Width 10m

(b) Width 13.5m

(d) Width 16m

(e) Width 20m

Figure 4.4 PLAXIS design charts of cohesion 5 kPa for different foundation widths with varying loads

(a) Width 7.5m

(b) Width 10m

(c) Width 13.5m

(d) Width 16m
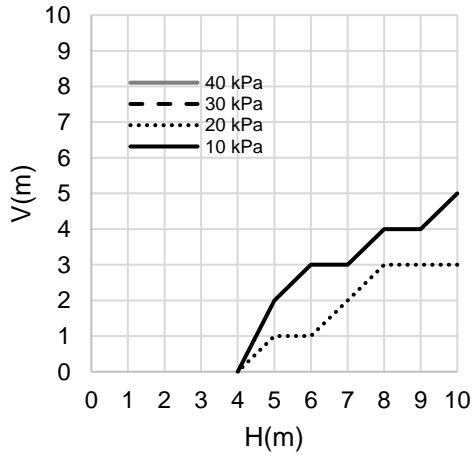
(e) Width 20m

Figure 4.5 PLAXIS design charts of cohesion 10 kPa for different
foundation widths with varying loads
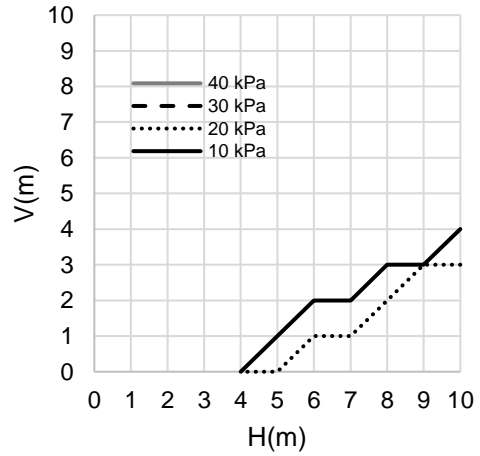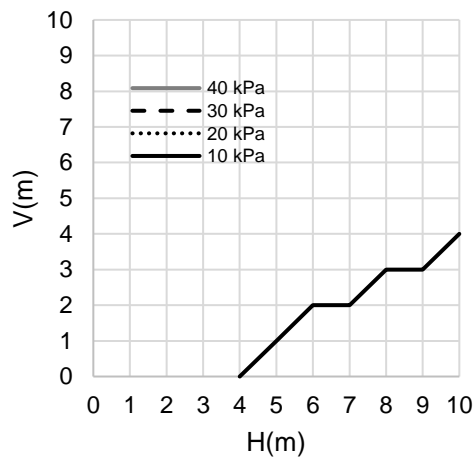
(a) Width 7.5m

(b) Width 10m

(c) Width 13.5m

(d) Width 16m

(e) Width 20m

Figure 4.6 PLAXIS design charts of cohesion 15 kPa for different
foundation widths with varying loads

Figure 4.7 PLAXIS design charts for 5kPa cohesion and 10 kPa load

(a) Load 10 kPa

(b) Load 20 kPa

Figure 4.8 PLAXIS design charts for 10kPa cohesion and varying loads

(a) Load 10kPa

(b) Load 20kPa

(c) Load 30kPa

Figure 4.9 PLAXIS design charts of cohesion 15kPa for different loads
with varying foundation widths

(a) Width 7.5m
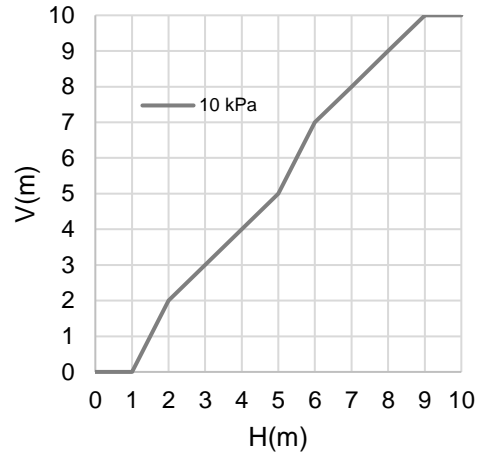
(b) Width 10m
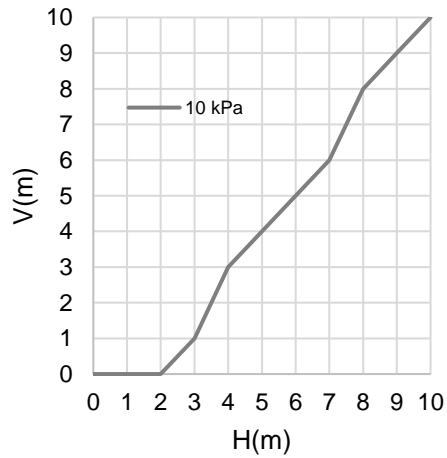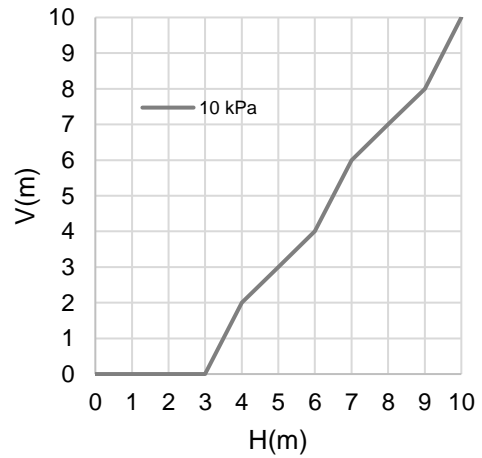
(c) Width 13.5m
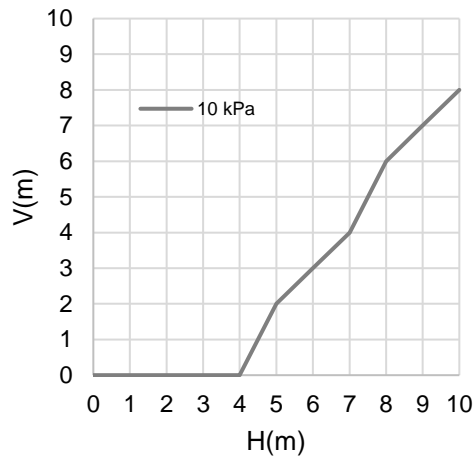
(d) Width 16m

(e) Width 20m

Figure 4.10 MLP design charts of cohesion 5 kPa for different
foundation widths with varying loads
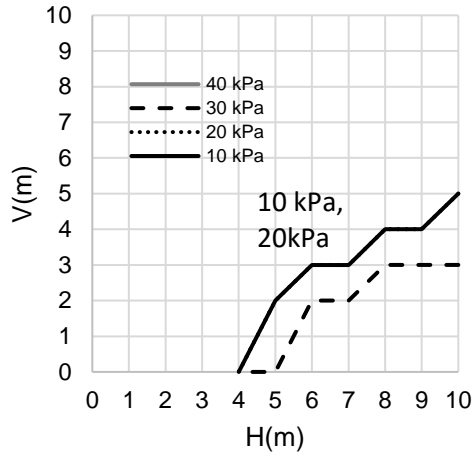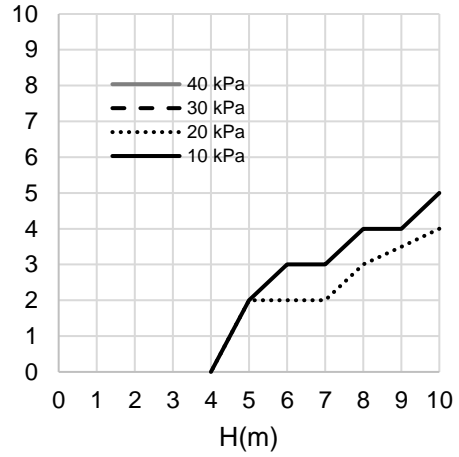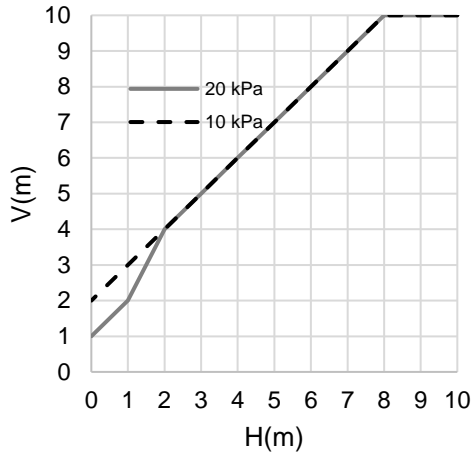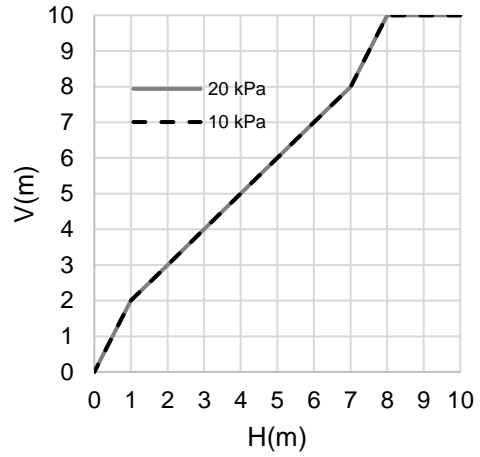
(a) Width 7.5m
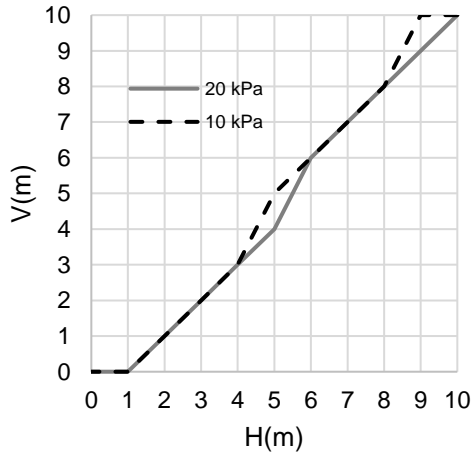
(b) Width 10m
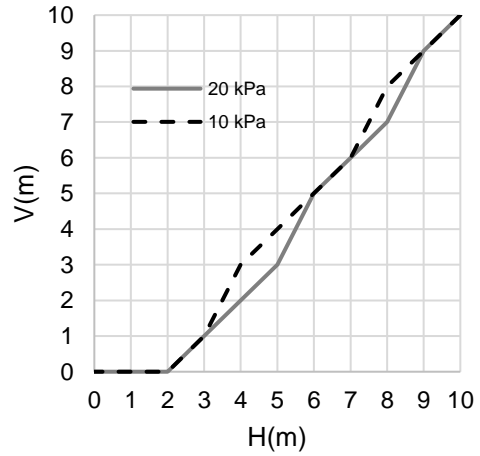
(c) Width 13.5m
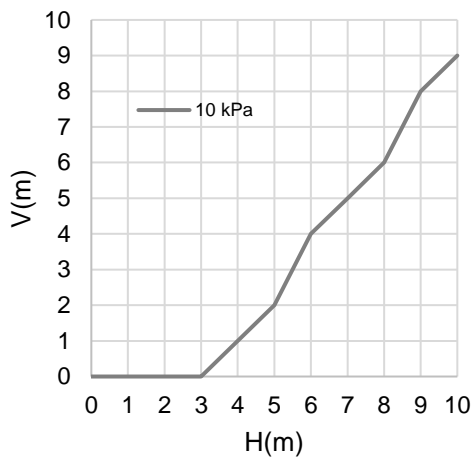
(d) Width 16m
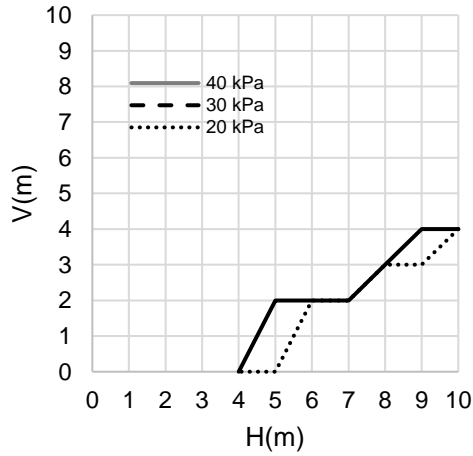
(e) Width 20m

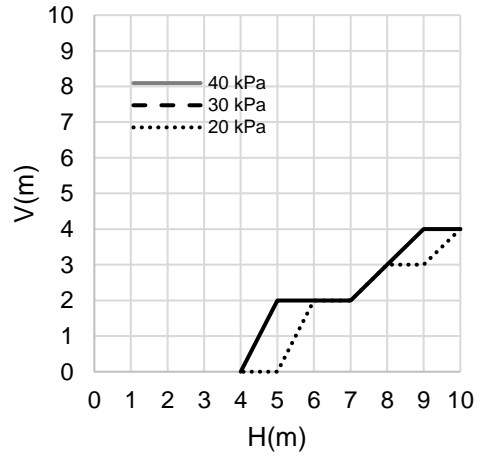Figure 4.11 MLP design charts of cohesion 10 kPa for different foundation widths with varying loads
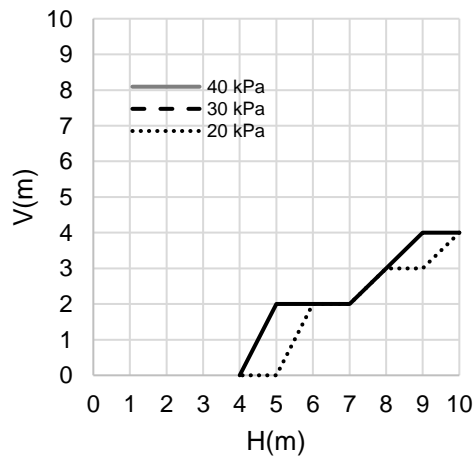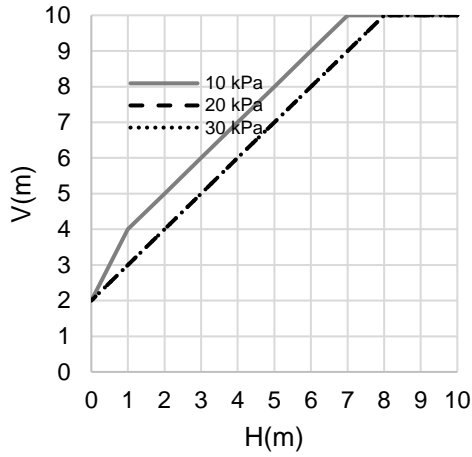
(a) Width 7.5m
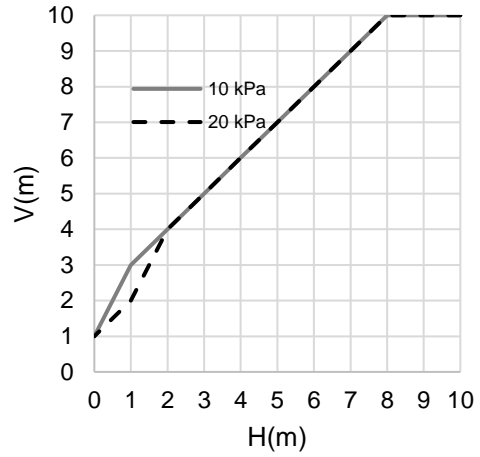
(b) Width 10m
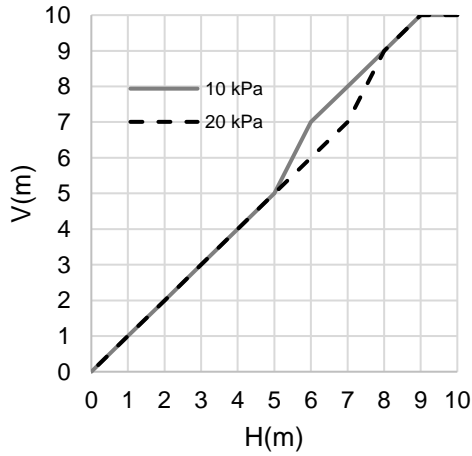
(c) Width 13.5m
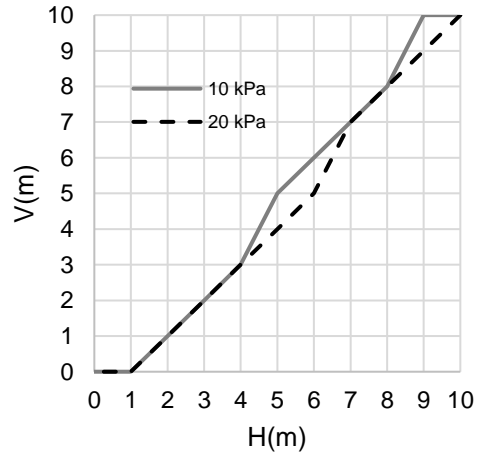
(d) Width 16m
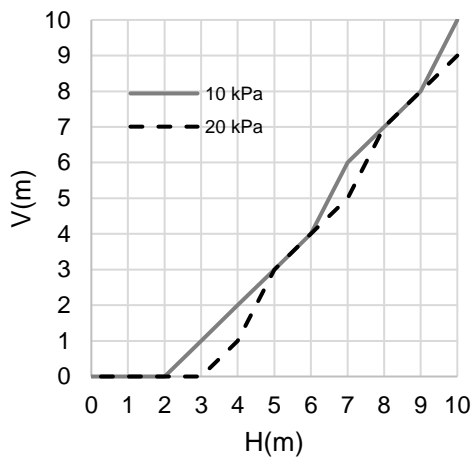
(e) Width 20m

Figure 4.12 MLP design charts of cohesion 15 kPa for different
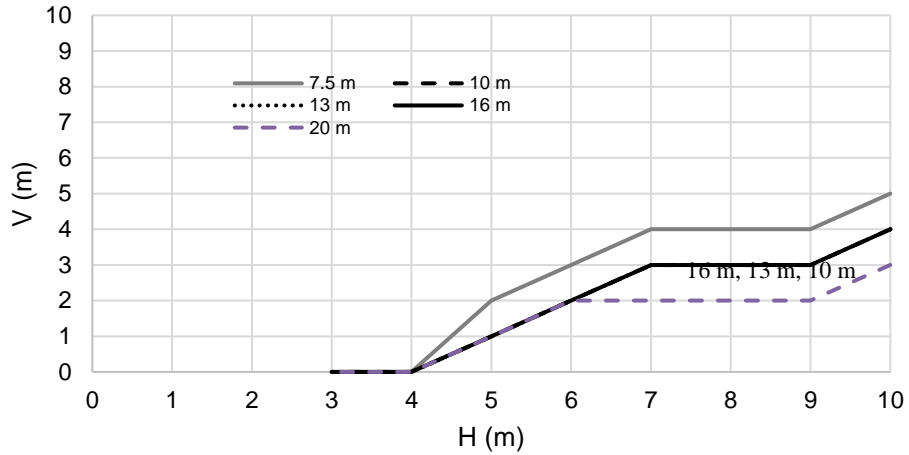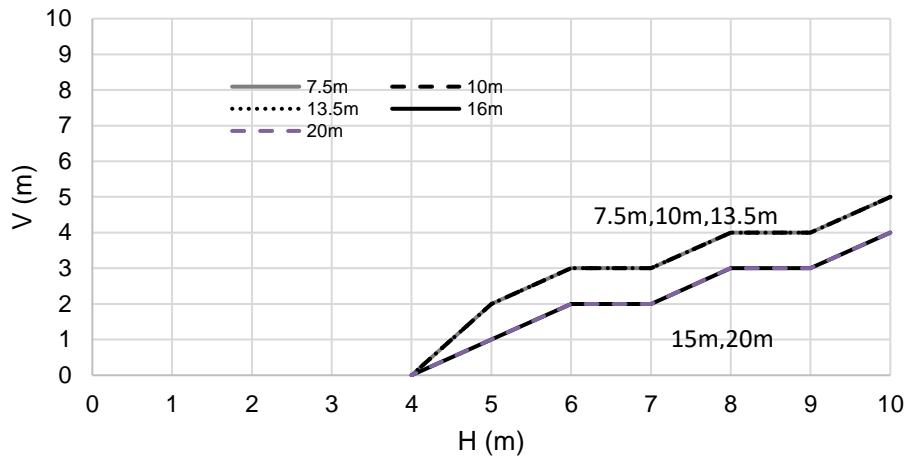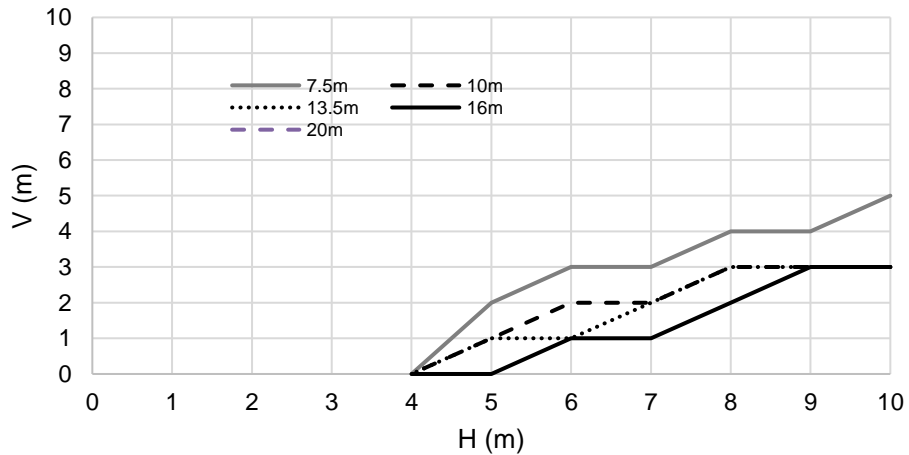foundation widths with varying loads
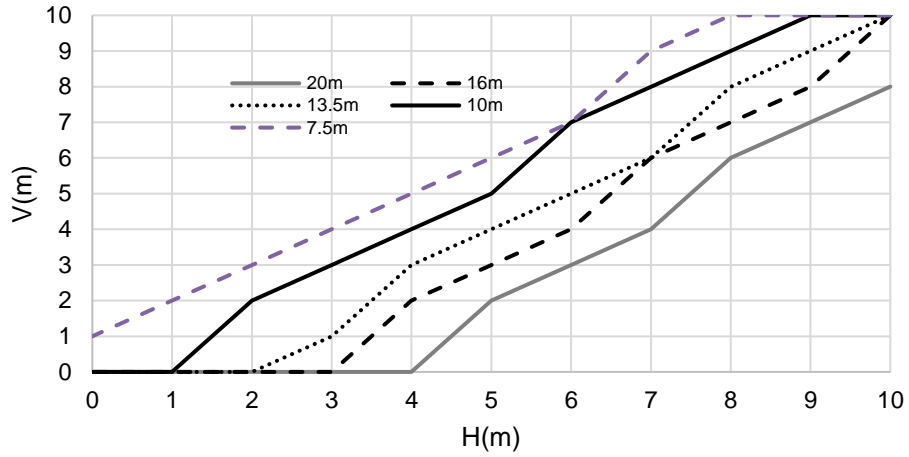
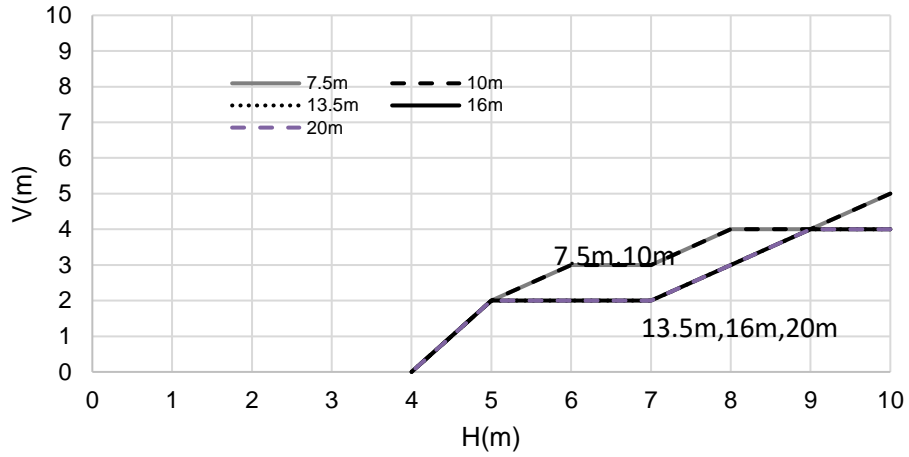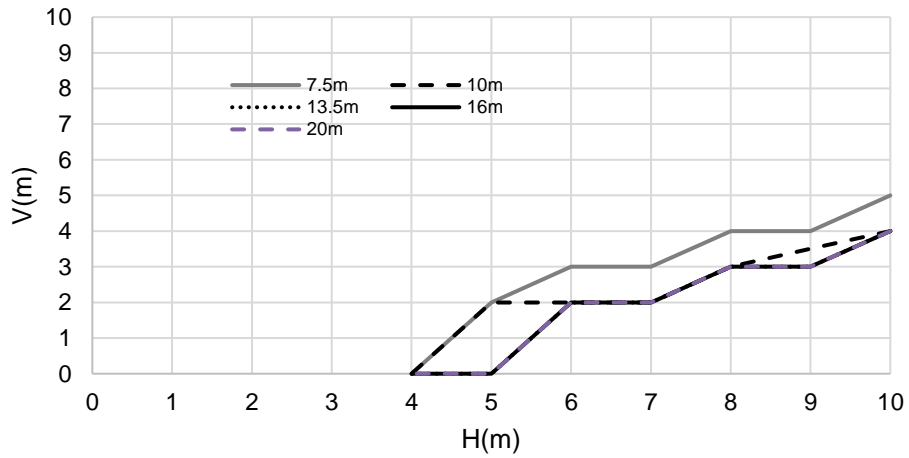Figure 4.13 MLP design charts for 5kPa cohesion and 10 kPa load
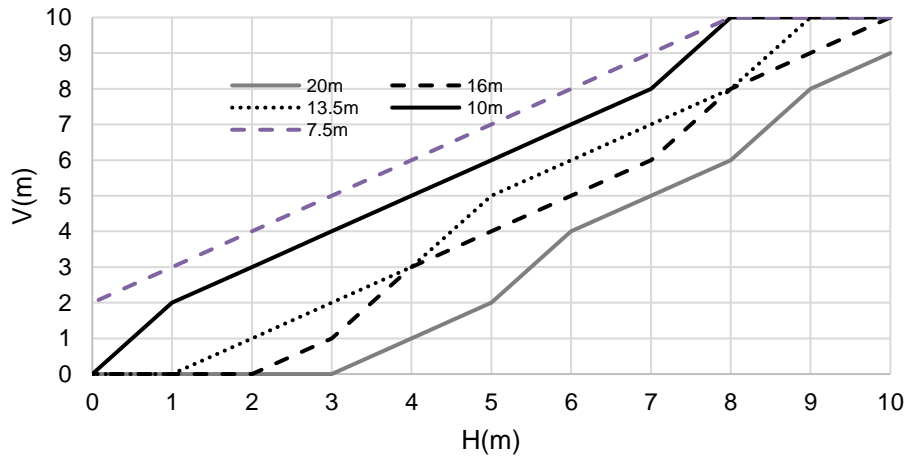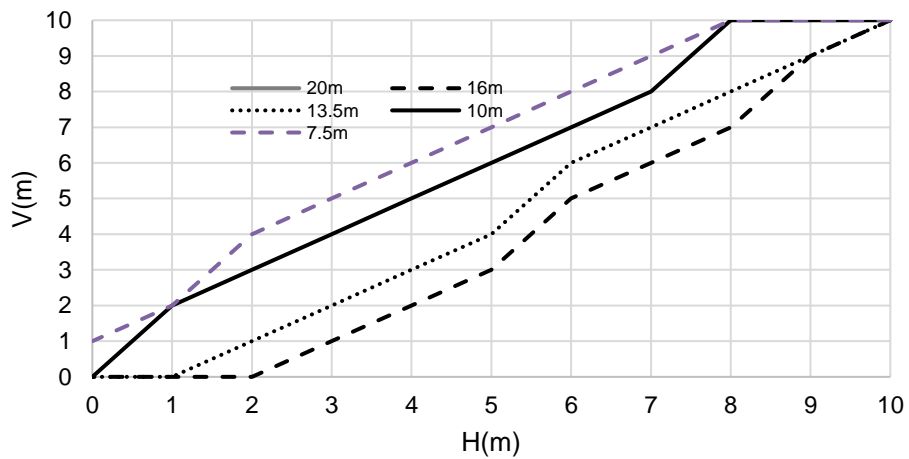
(a) Load 10kPa

(b) Load 20kPa

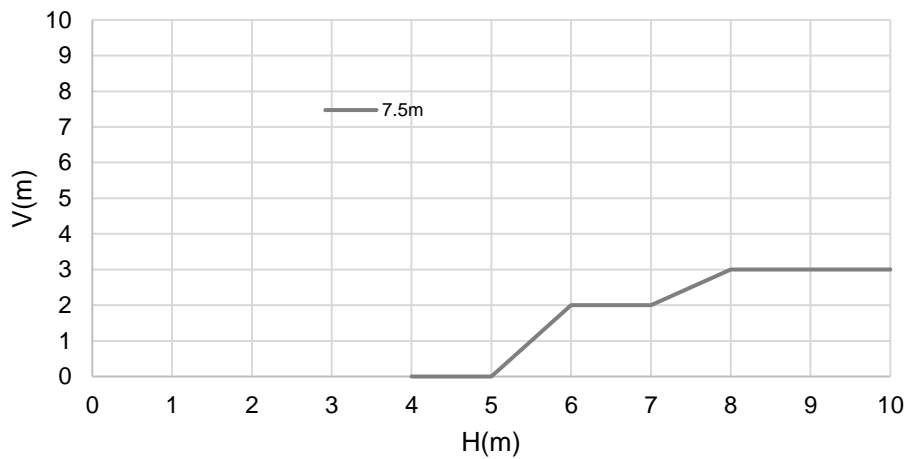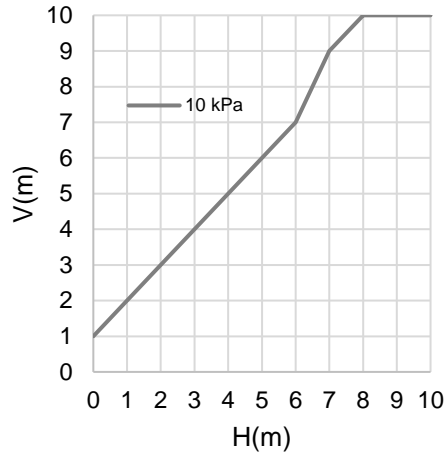Figure 4.14 MLP design charts for 10kPa cohesion and varying loads
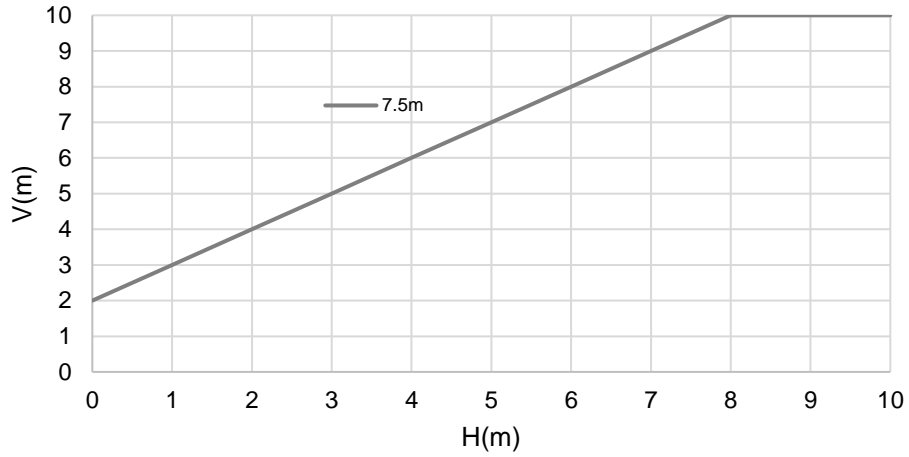
(a) Load 30kPa
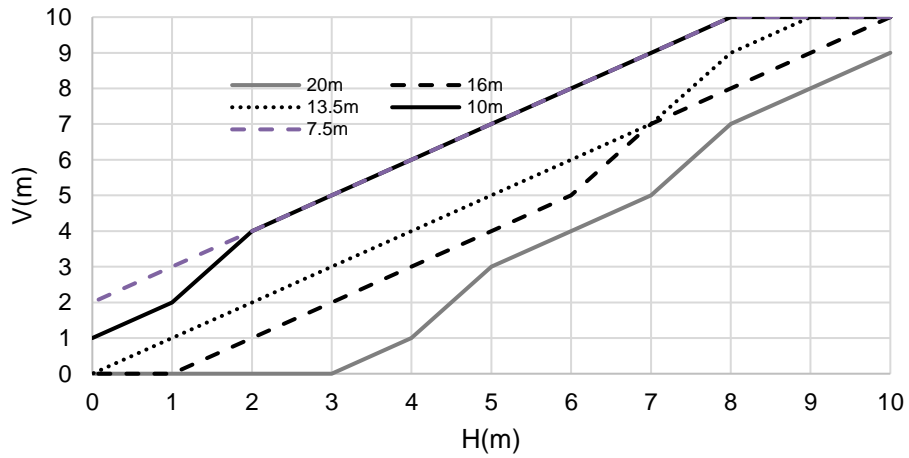
(b) Load 20kPa
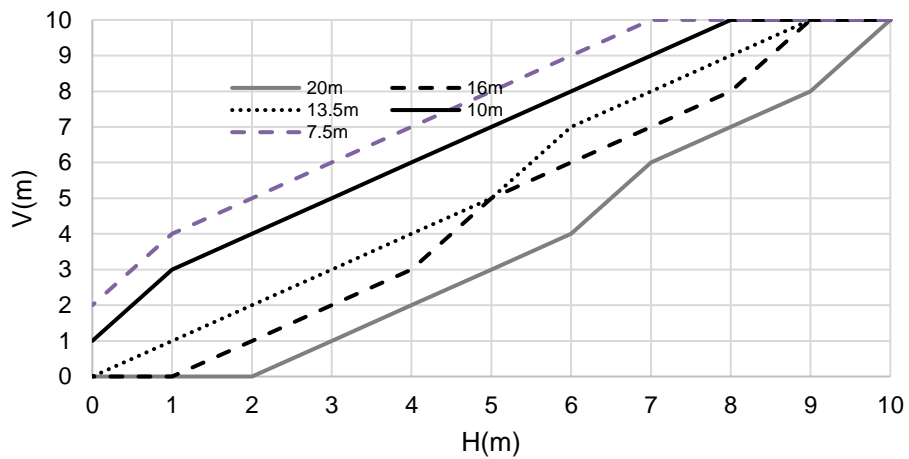
(c) Load 10kPa

Figure 4.15 MLP design charts of cohesion 15kPa for different loads
with varying foundation width

4.6 Validation of Design Charts

The design charts from PLAXIS and MLP were validated against the available case studies. The MLP design charts proved to be more accurate. The comparison is shown in figure 4.16. For modelling in PLAXIS, many assumptions had to be made which included assuming the soils were homogenous and Mohr-Columb criteria was applicable. On the contrary, MLP model was data driven which allowed little room for error based on the parameters considered for the study.
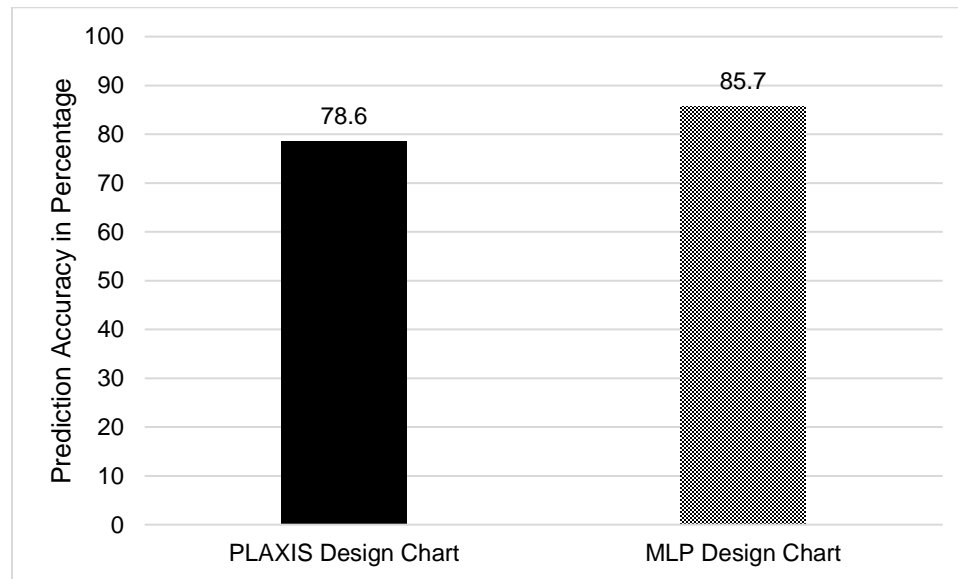
Figure 4.16 Prediction Accuracy of Design Charts

4.7 Binary Logistic Model

IBM Statistics software SPPS was used for Binary Logistic Regression to produce the following equation:

$$Z = -3.59(\gamma) + 0.426(c) + 5.681(E_{50}) - 1.819(B) - 0.519(L) + 4.575(H) - 5.365(V) + 83.559 \qquad 4.1$$

where γ is unit weight of soil in kN/m^3, c is cohesion of soil in kPa, E_{50} is elastic modulus of soil in MPa, B is foundation width in meters, L is load in kPa, H is horizontal distance from adjacent foundation in meters, and V is depth of excavation pit in meters and P is the probability of the safe combinations of H and V.

$$Z = ln \frac{P}{1-P} \qquad 4.2$$

47

The value of P is either 1 or 0. 1 indicates safe combinations of values while 0 indicates unsafe. The prediction accuracy of the equation is 95.8%.

4.8   Assumptions and Limitations

Following assumptions were made during the study.

1   Buildings under consideration are residential units.
2   Primary settlement had already occurred in the neighboring foundations.
3   The footings were close enough to be analyzed as mat foundations. (Jha & Jain, 2021)
4   Soils under consideration were soft soils.
5   Soils are homogenous.
6   No water table was encountered.

CHAPTER 5

CONCLUSIONS AND RECOMMENDATIONS

5.1   Conclusions

The following conclusions can be drawn from the study:

5.1.1   Database of precedents

The database of precedent cases was prepared by observing key characteristics of adjacent buildings next to which unsupported pits were being excavated. The buildings under consideration were residential units with foundation widths spanning from 7.5m to 20m. The loads under consideration ranged from 10 kPa to 40 kPa. The entire case was regarded safe for unsupported excavation if there was no settlement, distortion, or pit face failure otherwise it was regarded as unsafe. The data was collected using a survey form attached as Annex-A. Settlement and damage observations were made on site. A few in-situ tests were performed while soil samples were collected for laboratory testing. The database is attached as Annex-B. The soil testing concluded that all soil samples are soft soils since elastic modulus of all samples was less than 2Mpa. Hence the results from this study are only applicable to soft soils.

5.1.2   Soft Computing Models

Three machine learning models were used in the study i.e., Multilayer Perceptron (MLP), Decision Tree and Gene Expression Programming (GEP). The database collected was used for training and testing of the models. Multilayer Perceptron showed the best accuracy in predicting if a case of unsupported excavation was safe against settlement, distortion, or pit face failure. The accuracy of the model was 89%. The least accurate was decision tree with 67% accuracy. Soft computing models are not transparent, and the modelling process is complicated. The relationship between inputs and outputs is not accessible.

5.1.3   Sensitivity Analysis

Sensitivity analysis proposed by (Garson, 1991) and local sensitivity analysis with 10% perturbation in the input parameters was applied on MLP model. Garson (1991) method

determines the influence of each input parameter on the output with weights and biases of the layers whereas local sensitivity analysis determines the influence based on variance in output over small perturbations in the input factors. Both methods rendered elastic modulus and unit weight of the soil as the least influential input parameters out of the seven input parameters.

5.1.4 Design Charts

Design charts were made using PLAXIS and the MLP model. The five most influential parameters from the sensitivity analysis were taken as input parameters and their values were variated during modelling in PLAXIS. For each foundation width, load and cohesion value, an unsupported pit was excavated at 1-meter intervals till 10 meters depth at horizontal distance intervals of 1 meter till 10 meters. The same combinations were provided as input to the MLP model to make design charts. Following trends can be drawn from the design charts:

i.   It can be concluded that as cohesion values increased, the foundations of the same size and load were safe against more depths of unsupported foundations at smaller adjacent distances.

ii.   As the foundation size reduced, the foundations became more safer against deeper excavations at smaller adjacent distances.

iii. However, as load increased on the foundations of same size on soils with same cohesion values, the foundations became unsafe to deeper excavations at smaller adjacent distances.

iv.   For a particular cohesion and foundation width, MLP does not consider the effect of the load dominantly.

The PLAXIS and MLP design charts depict the same trends, however MLP design charts allow deeper unsupported excavations than PLAXIS design charts. The reason being that MLP model is data driven whereas in PLAXIS, the foundations were modelled using soil structure interaction models. Also, during PLAXIS modelling, many assumptions had to be made. Although PLAXIS design charts provided conservative limits of unsupported excavations, since MLP design charts are data driven, they take precedence. The MLP

design charts proved to be more accurate than PLAXIS design charts i.e., 85.7% and 78.5% respectively.

5.1.5 Binary logistic regression model

Binary logistic regression was applied to the database to predict if a particular combination of all 7 input parameters was safe for unsupported excavation. The equation proved to be 95.8% accurate.

5.1.6 Applicability

As mentioned earlier, the soil samples collected from the study area are soft soils and the buildings under consideration are residential units, therefore the machine learning model, design charts and binary logistic equation proposed in this study are only applicable to residential units constructed on soft soils. Unsupported excavations in medium stiff and hard soils do not pose serious threats adjacent structures. It is pertinent to mention that homogenous soil was considered, and water table was not taken into consideration for the study.

5.2 Recommendations

The study can be extended to widen the database of the case studies used in this research. Machine learning models other than the ones used in this study can also be explored. Non-homogenous soils and water-table can be taken into consideration for future studies. The study can also be extended to medium stiff soils. The foundation type considered in this study was mat foundation. Strip and isolated footings can also be taken into account. The design charts maybe automated.

ANNEX-A OPEN PIT EXCAVATION INDUCED DAMAGE SURVEY FORM

Open Pit Excavation Induced Damage Survey Form			
Address			Date
			Time
1	**Qualitative Damage Observations**		
a	Settlement Cracks	Yes/No	Description
b	Sagging / Hogging	Yes/No	Description
c	Pit Face Failure	Yes/No	Description
2	**Quantitative Damage Observations**		
a	Settlement		Comments
b	Angle of Distortion		Comments
3	**Building Parameters**		
a	Dimension Parallel to Excavation		Comments
b	Dimension Perpendicular to Excavation		Comments
c	No. of Storeys		Comments
d	Load		Comments
4	**Excavation Pit Parameters**		
a	Horizontal Distance from Building		Comments
b	Depth		Comments
5	**Soil Parameters**		
a	Unit Weight		Comments
b	Moisture Content		
c	Angle of Internal Friction		
d	Cohesion		

ANNEX-B DATABASE

Case No.	Unit Weight (kN/m³)	Cohesion (kPa)	E50 (MPa)	Foundation Width (m)	Load (kPa)	Adjacent Distance - H (m)	Excavation Depth - V (m)	Safe-1 Unsafe - 0
1	16	15	2	12	25.5	5	3	1
2	16	15	2	8	14.2	3	6	1
3	16	15	2	16	14.2	0	7	0
4	16	15	2	8	14.2	2	7	0
5	16	15	2	7	37.0	2	6	0
6	16	15	2	7	37.0	2	6	0
7	16	15	2	16	14.2	0	4	0
8	15	12	2	10	28.7	0	6	0
9	14	5	1	13	23.5	0	9	0
10	14	5	1	14	38.2	3	3	0
11	12	9	2	10	33.8	6	10	0
12	12	9	2	10	35.4	2	9	0
13	12	9	2	14	24.9	6	8	1
14	12	9	2	11	50.0	1	3	0
15	14	25	2	18	11.4	0	5	0
16	14	25	2	20	21.4	3	4	0

Case No.	Unit Weight (kN/m³)	Cohesion (kPa)	E50 (MPa)	Foundation Width (m)	Load (kPa)	Adjacent Distance - H (m)	Excavation Depth - V (m)	Safe-1 Unsafe - 0
17	14	25	2	20	21.4	2	4	0
18	14	25	2	14	30.1	2	4	1
19	14	25	2	14	30.1	1	4	1
20	14	25	2	14	22.9	1	3	1
21	14	25	2	10	28.7	0	2	1
22	14	25	2	10	45.4	4	6	0
23	14	25	2	9	27.4	0	5	0
24	14	25	2	10	45.4	5	6	1
25	16	26	3	15	11.1	1	6	0
26	16	26	3	16	11.5	0	4	0
27	16	26	3	16	11.5	2	4	1
28	16	26	3	16	11.5	2	4	1
29	16	26	3	16	11.6	3	3	1
30	16	26	3	16	11.6	3	3	1
31	16	26	3	12	14.5	2	6	1
32	16	26	3	12	15.1	3	6	1
33	16	26	3	8	14.9	0	6	0
34	16	26	3	8	29.9	2	6	1
35	16	26	3	8	14.9	3	5	1

Case No.	Unit Weight (kN/m³)	Cohesion (kPa)	E50 (MPa)	Foundation Width (m)	Load (kPa)	Adjacent Distance - H (m)	Excavation Depth - V (m)	Safe-1 Unsafe - 0
36	16	25	3	17	11.2	5	4	1
37	16	25	3	20	11.3	10	10	1
38	16	25	3	30	28.5	0	2	0
39	16	25	3	20	31.0	4	2	1
40	16	25	3	20	11.3	2	2	1
41	17	32	4	8	29.2	2	3	1
42	17	32	4	15	24.5	5	6	1
43	17	32	4	13	25.4	3	6	1
44	17	32	4	13	25.4	3	6	1

ANNEX-C COMBINATIONS FOR MODELLING IN PLAXIS

Sr. No.	Cohesion (kPa)	Foundation Width (m)	Load (kPa)	Sr. No.	Cohesion (kPa)	Foundation Width (m)	Load (kPa)	Sr. No.	Cohesion (kPa)	Foundation Width (m)	Load (kPa)
1	5	7.6	10	24	10	7.6	40	47	15	10	30
2	5	7.6	20	25	10	10	10	48	15	10	40
3	5	7.6	30	26	10	10	20	49	15	13.5	10
4	5	7.6	40	27	10	10	30	50	15	13.5	20
5	5	10	10	28	10	10	40	51	15	13.5	30
6	5	10	20	29	10	13.5	10	52	15	13.5	40
7	5	10	30	30	10	13.5	20	53	15	16	10
8	5	10	40	31	10	13.5	30	54	15	16	20
9	5	13.5	10	32	10	13.5	40	55	15	16	30
10	5	13.5	20	33	10	16	10	56	15	16	40
11	5	13.5	30	34	10	16	20	57	15	20	10
12	5	13.5	40	35	10	16	30	58	15	20	20
13	5	16	10	36	10	16	40	59	15	20	30
14	5	16	20	37	10	20	10	60	15	20	40
15	5	16	30	38	10	20	20				
16	5	16	40	39	10	20	30				
17	5	20	10	40	10	20	40				
18	5	20	20	41	15	7.6	10				
19	5	20	30	42	15	7.6	20				
20	5	20	40	43	15	7.6	30				
21	10	7.6	10	44	15	7.6	40				
22	10	7.6	20	45	15	10	10				
23	10	7.6	30	46	15	10	20				

REFERENCES

Al-Kodmany, K. (2012). The Logic of Vertical Density: Tall Buildings in the 21st Century City. *International Journal of High-Rise Buildings*, *1*(2), 131–148. https://doi.org/10.21022/IJHRB.2012.1.2.131

Alessandri, C., Garutti, M., Mallardo, V., & Milani, G. (2015). Crack patterns induced by foundation settlements: Integrated analysis on a renaissance masonry palace in Italy. *International Journal of Architectural Heritage*, *9*(2), 111–129. https://doi.org/10.1080/15583058.2014.951795

Aljorany, A. N., & Al-qaisee, G. S. (2018). Field observations and finite element 3-D analysis of soil displacements close to unsupported excavation. *MATEC Web of Conferences*, *01029*, 3–8.

Aly, M. (2005). Survey on multiclass classification methods. *Neural Network*, *November*, 1–9. https://www.cs.utah.edu/~piyush/teaching/aly05multiclass.pdf

Antinoro, C., Arnone, E., & Noto, L. V. (2017). The use of soil water retention curve models in analyzing slope stability in differently structured soils. *Catena*, *150*, 133–145. https://doi.org/10.1016/j.catena.2016.11.019

ASTM D1556-00. (2016). Standard Test Method for Density and Unit Weight of Soil in Place by the Sand-Cone Method. In *ASTM International, West Conshohocken, PA, American Society for Testing and Materials*. https://doi.org/10.1520/D1556

ASTM D2166. (2016). Standard Test Method for Unconfined Compressive Strength of Cohesive Soil 1. *ASTM International, West Conshohocken, PA, American Society for Testing and Materials*, *January*, 1–7. https://doi.org/10.1520/D2166

ASTM D2487. (2020). D2487 "Standard Practice for Classification of Soils for Engineering Purposes (Unified Soil Classification System)." *ASTM International, West Conshohocken, PA, American Society for Testing and Materials*. https://doi.org/10.1520/D2487-17E01.2

ASTM D4318. (2018). Standard Test Methods for Liquid Limit, Plastic Limit, and Plasticity Index of Soils. *ASTM International, West Conshohocken, PA, American*

Society for Testing and Materials, *04*(March 2010), 1–14. https://doi.org/10.1520/D4318-17E01.

ASTM D4944-18. (2018). Standard Test Method for Field Determination of Water (Moisture) Content of Soil by the Calcium Carbide Gas Pressure Tester Method 1. In *ASTM International, West Conshohocken, PA, American Society for Testing and Materials* (Vol. 04). https://doi.org/10.1520/D4944-18.1.5

ASTM D6913. (2021). Standard Test Methods for Particle-Size Distribution (Gradation) of Soils Using Sieve. *ASTM International, West Conshohocken, PA, American Society for Testing and Materials*. https://doi.org/10.1520/D6913

ASTM D7928. (2021). Standard Test Method for Particle-Size Distribution (Gradation) of Fine-Grained Soils Using the Sedimentation (Hydrometer) Analysis. *ASTM International, West Conshohocken, PA, American Society for Testing and Materials*, 1–25. https://doi.org/10.1520/D7928-21E01

Bakr, R. M. (2019). The Impact of the Unsupported Excavation on the Boundary of the Active Zone in Medium, Stiff and Very Stiff Clay. *Journal of Civil & Environmental Engineering*, *9*(1), 1–9. https://doi.org/10.4172/2165-784X.1000327

Batta, M. (2020). Machine Learning Algorithms - A Review . *International Journal of Science and Research (IJ*, *9*(1), 381-undefined. https://doi.org/10.21275/ART20203995

Bay, S. D. (1999). Nearest neighbor classification from multiple feature subsets. *Intelligent Data Analysis*, *3*(3), 191–209. https://doi.org/10.3233/IDA-1999-3304

Bond, A. J., Bernd, S., Scarpelli, G., & Orr, T. L. L. (2013). BS EN 1997-1:2004+A1:2013 Eurocode 7: Geotechnical Design - Part 1: General Rules. In *BSI Standards Limited* (Vol. 87, Issue 18). https://doi.org/10.2788/3398

Bonshor, R., Bonshor, L., & Sadgrove, R. (1998). Cracking in Building. *Structural Survey*, *16*(2). https://doi.org/10.1108/ss.1998.11016bae.007

Bowles, J. E. (1996). Foundation Analysis and Design,. In *5th ed., McGraw-Hill, New York.* (pp. 162–165).

Bowles, J. E. (1997). *Foundation Analysis and Design* (5th ed.).

Brennan, G., Oh, W., & Nasir, O. (2020). *Experimental Study on the Critical Height of an Unsupported Vertical Cut*.

Burland, J. B., & Wroth, C. P. (1974). Settlement of buildings and associated damage. *Settlement of Structures, Proceedings of the Conference of the British Geotechnical Society*, *April*, 611–654.

Commend, S., Wattel, S., Hennebert, J., Kuonen, P., & Vulliet, L. (2019). Prediction of Unsupported Excavtions Behaviour with Machine Learning Techniques. *XIV International Conference on Computational Plasticity. Fundamentals and Applications COMPLAS 2019*, 529–535.

Cortes, C., & Vladimir, V. (1995). Support-vector networks. *Machine Learning*. https://doi.org/10.1109/64.163674

Dabbaghi, F., Rashidi, M., Nehdi, M. L., Sadeghi, H., Karimaei, M., Rasekh, H., & Qaderi, F. (2021). Experimental and informational modeling study on flexural strength of eco-friendly concrete incorporating coal waste. *Sustainability (Switzerland)*, *13*(13). https://doi.org/10.3390/su13137506

Dalgic, K. D., Hendriks, M. A. N., & Ilki, A. (2018). Building response to tunnelling- and excavation-induced ground movements: using transfer functions to review the limiting tensile strain method. *Structure and Infrastructure Engineering*, *14*(6), 766–779. https://doi.org/10.1080/15732479.2017.1360364

Daud, K. A. (2012). Interference of shallow multiple strip footings on sand. *The Iraqi Journal For Mechanical And Material Engineering*, *12*(3), 492–507. http://www.iqjmme.com/papers/jjou_paper_2016_51642590.pdf

Dmochowski, G., & Szolomicki, J. (2021). Technical and structural problems related to the interaction between a deep excavation and adjacent existing buildings. *Applied Sciences (Switzerland)*, *11*(2), 1–19. https://doi.org/10.3390/app11020481

Ercio, T., Hipólito, S., Humberto, R., John, M., José M., S., Márcio, C., Oscar, P., Paulo B., L., Romeu S., V., & Rui, S. (2006). *Defects in masonry walls - Guidance on*

cracking: Identification, Prevention & Repair. May 2015. http://www.hms.civil.uminho.pt/arq/fich/CIB_403.pdf

Fellenius, W. (1927). *Erdstatische Berechnungen* (Revised Ed). W. Ernst u. Sons, Berlin.

Garson, G. D. (1991). Interpreting Neural Network Connection Weights. *AI Expert*, *6*, 47–51.

Giardina, G. (2013). *Modelling of Settlement Induced Building Damage*. TU Delft.

Grimm, T. C. (1988). *Masonry-Cracks-A-Review-of-the-Literature-Grimm.pdf* (pp. 257–280).

Hamby, D. M. (1994). A review of techniques for parameter sensitivity analysis of environmental models. *Environmental Monitoring and Assessment*, *32*(2), 135–154.

Hu, J., & Ma, F. (2018). Failure Investigation at a Collapsed Deep Open Cut Slope Excavation in Soft Clay. *Geotechnical and Geological Engineering*, *36*(1), 665–683. https://doi.org/10.1007/s10706-017-0337-2

Hussain, K., He, Z., Ahmad, N., Iqbal, M., & Taskheer mumtaz, S. M. (2019). Green, lean, Six Sigma barriers at a glance: A case from the construction sector of Pakistan. *Building and Environment*, *161*(March). https://doi.org/10.1016/j.buildenv.2019.106225

Irfan, M., Akbar, A., Aziz, M., & Khan, A. H. (2013). A Parametric Study on Stability of Open Excavations in Alluvial Soils of Lahore District, Pakistan. *Geotechnical and Geological Engineering*, *31*(2), 729–738. https://doi.org/10.1007/s10706-013-9623-9

Islamabad Residential Sector Zoning-Building Control Regulations. (2005).

Javed, M. F., Amin, M. N., Shah, M. I., Khan, K., Iftikhar, B., Farooq, F., Aslam, F., Alyousef, R., & Alabduljabbar, H. (2020). Applications of gene expression programming and regression techniques for estimating compressive strength of bagasse ash based concrete. *Crystals*, *10*(9), 1–17. https://doi.org/10.3390/cryst10090737

Karl, C. (1866). *Die graphische Statik*. Zürich : Meyer & Zeller, 1866.

Kézdi, Á., & Réthati, L. (1974). *Handbook of soil mechanics*. Amsterdam: Elsevier.

Kohestani, V. R., Vosoghi, M., Hassanlourad, M., & Fallahnia, M. (2017). Bearing Capacity of Shallow Foundations on Cohesionless Soils: A Random Forest Based Approach. *Civil Engineering Infrastructures Journal*, *50*(1), 35–49. https://doi.org/10.7508/ceij.2017.01.003

Lee, C. J., & Hsiung, T. K. (2009). Sensitivity analysis on a multilayer perceptron model for recognizing liquefaction cases. *Computers and Geotechnics*, *36*(7), 1157–1163. https://doi.org/10.1016/j.compgeo.2009.05.002

Mahamat, A. A., Boukar, M. M., Ibrahim, N. M., Stanislas, T. T., Linda Bih, N., Obianyo, I. I., & Savastano, H. (2021). Machine learning approaches for prediction of the compressive strength of alkali activated termite mound soil. *Applied Sciences (Switzerland)*, *11*(11). https://doi.org/10.3390/app11114754

Mehmood, E., Tariq, K. A., Khan, S. U., & Raza, A. (2018). Case study of detailed settlement analysis of an old residential building within lahore fort, pakistan. *Proceedings of the Pakistan Academy of Sciences: Part A*, *55*(3), 1–9.

Mohafezatkar Sereshkeh, A., & Jamshidi Chenari, R. (2017). Induced Settlement Reduction of Adjacent Masonry Building in Residential Constructions. *Civil Engineering Journal*, *3*(7), 450–462. https://doi.org/10.28991/cej-2017-00000104

Nangan, A. P., Ganiron, T. U., & Martinez, D. T. (2017). Concrete Foundation Systems and Footings. *World Scientific News*, *80*(July), 1–17.

Ngoc, D. M., Nu, N. T., Tinh, D. M., van Loi, B., & Huong, N. T. T. (2020). An analytical model for residual stress prediction in rebound deformation of the foundation pit. *Journal of Applied Science and Engineering*, *23*(4), 661–668. https://doi.org/10.6180/jase.202012_23(4).0010

Obrzud, R. (2010). *The hardening soil model: A practical guidebook*. Zace Services Ltd, Software engineering. Lausanne.

Ouyang, B., Song, Y., Li, Y., Wu, F., Yu, H., Wang, Y., Yin, Z., Luo, X., Sant, G., & Bauchy, M. (2021). Using machine learning to predict concrete's strength: Learning

from small datasets. *Engineering Research Express*, *3*(1). https://doi.org/10.1088/2631-8695/abe344

Prat, M., Bisch, E., Millard, A., Mestat, P., & Cabot, G. (1995). *The modeling of the structures (La modelisation des ouvrages).*

Richard, A., Oh, W. T., & Brennan, G. (2019). Estimating critical height of unsupported trenches in vadose zone. *Canadian Geotechnical Journal*, *58*(1), 66–82.

Ruiz-Jaramillo, J., Mascort-Albea, E., & Jaramillo-Morilla, A. (2016). Proposed methodology for measurement, survey and assessment of vertical deformation of structures. *Structural Survey*, *34*(3), 276–296. https://doi.org/10.1108/SS-02-2016-0006

S. B. Kotsiantis. (2007). Supervised Machine Learning: A Review of Classification Techniques. *Informatica (Slovenia)*, *31*, 249–268. https://doi.org/10.1007/s10751-016-1232-6

Sameen, M. I., Pradhan, B., & Lee, S. (2019). Self-Learning Random Forests Model for Mapping Groundwater Yield in Data-Scarce Areas. *Natural Resources Research*, *28*(3), 757–775. https://doi.org/10.1007/s11053-018-9416-1

Singh, A., Thakur, N., & Sharma, A. (2016). A review of supervised machine learning algorithms. *Proceedings of the 10th INDIACom; 2016 3rd International Conference on Computing for Sustainable Global Development, INDIACom 2016*, 1310–1315.

Sivakrishna, A., Adesina, A., Awoyera, P. O., & Kumar, K. R. (2020). Green concrete: A review of recent developments. *Materials Today: Proceedings*, *27*, 54–58. https://doi.org/10.1016/j.matpr.2019.08.202

Strózyk, J., & Tankiewicz, M. (2016). The elastic undrained modulus Eu50 for stiff consolidated clays related to the concept of stress history and normalized soil properties. *Studia Geotechnica et Mechanica*, *38*(3), 67–72. https://doi.org/10.1515/sgem-2016-0025

Terzaghi, K. (1943). *Theoretical Soil Mechanics*. John Wiley and Sons, New York.

Toderian, B. (2011). The Case for Density in Sustainable Cities. *Urban Land, Green*.

Truty, A., & Obrzud, R. (2011). *Guidebook, The Hardening soil model–a practical*. Zace Services Ltd, Software engineering. Lausanne.

U.S Department of Labor, O. S. and health A. (2015). *Trenching and Excavation Safety OSHA 2226-10R 2015*. 21. https://www.osha.gov/Publications/osha2226.pdf

Wang, Z. yu, Gu, D. ming, & Zhang, W. gang. (2020). Influence of excavation schemes on slope stability: A DEM study. *Journal of Mountain Science*, *17*(6), 1509–1522. https://doi.org/10.1007/s11629-019-5605-6

Wolkenhauer, O., Wellstead, P., Cho, K. H., & Ingalls, B. (2008). Sensitivity analysis: from model parameters to system behaviour. *Essays in Biochemistry*, *45*, 177194.

Zain, M., Usman, M., Farooq, S. H., & Mehmood, T. (2019). Seismic Vulnerability Assessment of School Buildings in Seismic Zone 4 of Pakistan. *Advances in Civil Engineering*, *2019*. https://doi.org/10.1155/2019/5808256

Zhang, Q. (2020). Deformation analysis of deep foundation pit excavation in China under time-space effect. *Geotechnical Research*, *7*(3), 146–152. https://doi.org/10.1680/jgere.20.00009

Zhang, W., Li, H., Li, Y., Liu, H., Chen, Y., & Ding, X. (2021). Application of deep learning algorithms in geotechnical engineering: a short critical review. In *Artificial Intelligence Review* (Vol. 54, Issue 8). Springer Netherlands. https://doi.org/10.1007/s10462-021-09967-1

Zhang, X., Yang, J., Zhang, Y., & Gao, Y. (2018). Cause investigation of damages in existing building adjacent to foundation pit in construction. *Engineering Failure Analysis*, *83*(September 2017), 117–124. https://doi.org/10.1016/j.engfailanal.2017.09.016